HHS Public Access

Author manuscript

J Med Chem. Author manuscript; available in PMC 2022 February 12.

Published in final edited form as:

J Med Chem. 2021 August 12; 64(15): 11045–11062. doi:10.1021/acs.jmedchem.1c00439.

Exploration and Biological Evaluation of Basic Heteromonocyclic Propanamide Derivatives as SARDs for the Treatment of Enzalutamide-Resistant Prostate Cancer

Yali He,
Department of Pharmaceutical Sciences, University of Tennessee Health Science Center, Memphis, Tennessee 38163, United States

Dong-Jin Hwang,
Department of Pharmaceutical Sciences, University of Tennessee Health Science Center, Memphis, Tennessee 38163, United States

Suriyan Ponnusamy,
Department of Medicine, College of Medicine, University of Tennessee Health Science Center, Memphis, Tennessee 38163, United States

Thirumagal Thiyagarajan,
Department of Medicine, College of Medicine, University of Tennessee Health Science Center, Memphis, Tennessee 38163, United States

Michael L. Mohler,
Department of Pharmaceutical Sciences, University of Tennessee Health Science Center, Memphis, Tennessee 38163, United States

Ramesh Narayanan,
Department of Medicine, College of Medicine, University of Tennessee Health Science Center, Memphis, Tennessee 38163, United States

Duane D. Miller
Department of Pharmaceutical Sciences, University of Tennessee Health Science Center, Memphis, Tennessee 38163, United States

Abstract

A series of propanamide derivatives were designed, synthesized, and pharmacologically characterized as selective androgen receptor degraders (SARDs) and pan-antagonists that exert

Corresponding Author: Duane D. Miller – Department of Pharmaceutical Sciences, University of Tennessee Health Science Center, Memphis, Tennessee 38163, United States; Phone: (+1)-901-448-6026; dmiller@uthsc.edu; Fax: (+1)-901-448-3446.

Author Contributions

The manuscript was written through contributions of all authors. All authors have given approval to the final version of the manuscript.

Supporting Information

The Supporting Information is available free of charge at https://pubs.acs.org/doi/10.1021/acs.jmedchem.1c00439.
Additional information on compound characterization; and additional biological experiments and figures (PDF)
Molecular formula strings (CSV)

Complete contact information is available at: https://pubs.acs.org/10.1021/acs.jmedchem.1c00439

The authors declare no competing financial interest.

a broad-scope androgen receptor (AR) antagonism. Incorporating different basic heteromonocyclic B-ring structural elements in the common A-ring–linkage–B-ring nonsteroidal antiandrogen general pharmacophore contributed to a novel scaffold of small molecules with SARD and pan-antagonist activities even compared to our recently published AF-1 binding SARDs such as UT-69 (**11**), UT-155 (**12**), and UT-34 (**13**). Compound **26f** exhibited inhibitory and degradation effects in vitro in a wide array of wtAR, point mutant, and truncation mutant-driven prostate cancers (PCs). Further, **26f** inhibited tumor cell growth in a xenograft model composed of enzalutamide-resistant (EnzR) LNCaP cells. These results demonstrate an advancement toward the development of novel SARDs and pan-antagonists with efficacy against EnzR prostate cancers.

Graphical Abstract

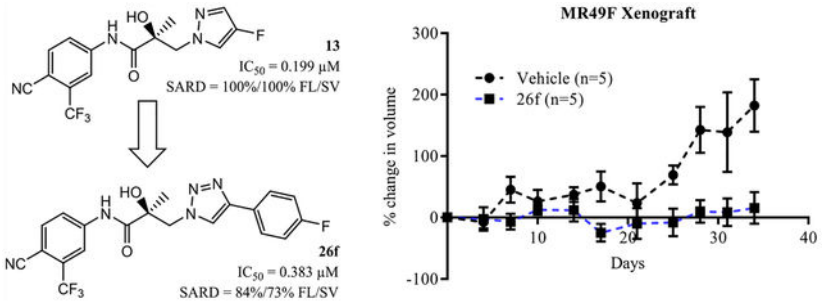

INTRODUCTION

Prostate cancer (PC) is the most common cancer and the second leading cause of cancer-related deaths, after lung cancer, in American men.[1,2] Since PC depends on the activation of androgen receptor (AR) signaling for its development, progression, growth, and survival, the AR represents the primary therapeutic target. Blockage of the androgen signal is very important and proven to be effective for PC treatment.[3–5] In addition to surgical or chemical castration by gonadotropin-releasing hormone (GnRH) analogues, AR antagonists, such as cyproterone acetate (**1**),[6,7] flutamide (**2**),[8] bicalutamide (**3**),[9] nilutamide (**4**), enzalutamide (**5**),[10] apalutamide (**6**),[11,12] or darolutamide (**7**),[13,14] or the androgen synthesis inhibitor abiraterone acetate (**8**) plus prednisone (Figure 1)[15] have been used to block the androgen signal. AR antagonists, in combination with castration, demonstrate significant effects by blocking adrenal androgen signals as well as suppressing transient testosterone increase induced by GnRH analogues, with the trend toward their use earlier in the disease to more effectively delay disease progression.[16–18]

Although the exact mechanisms of progression to castration-resistant PC (CRPC) are not always known, numerous contributing factors to the emergence of CRPC have been demonstrated and include (1) compensatory production of intratumoral androgens (e.g., 5α-dihydrotestosterone (DHT) synthesized from adrenal precursors);[3,19,20] (2) AR gene amplifications and overexpression;[21–23] (3) AR ligand binding domain (LBD) point mutations;[22,24,25] (4) alterations in the expression of coregulatory proteins;[26,27] (5) ligand-independent activation of AR;[28–32] (6) constitutively active truncated AR splice variants (AR SVs);[33] and (7) induction of intracrine androgen synthesis.[34–36] Despite resistance to

AR antagonist therapies in CRPC, AR signaling continues to be important for tumor growth and disease progression. Correspondingly, the development of AR antagonists with novel mechanisms of action to inhibit the AR-axis is urgently needed in hormone-resistant PCs.[37]

In the course of exploring novel antiandrogens, our research group has reported the discovery and characterization of UT-69 (**11**) and UT-155 (**12**) as AR antagonists and degraders that selectively inhibit tumor growth and degrade both full-length AR and AR splice variants (AR SVs).[38] Our laboratory also reported a series of aryl indol-1-yl propanamides and aryl indolin-1-yl propanamides as selective androgen receptor degraders (SARDs)[39] and most recently reported an aryl pyrazol-1-yl propanamide (**13**; termed UT-34 therein) as an orally available SARD.[40] Compounds **11** and **12** bind to both the N-terminal domain (NTD) at the transcriptional activation units (Tau)-1 and −5 (Tau-1 and Tau-5) of the activation function-1 (AF-1) domain and competitively bind the LBD, while compound **13** was demonstrated to bind the same Tau-1 and Tau-5 NTD sites, but it does not or very weakly binds the LBD (Figure 2).[40]

In the A-ring–linkage–B-ring general pharmacophore in Figure 2, the electron-deficient aromatic A-ring substituted by electron-withdrawing groups is required for the AR binding and functional activity (agonist or antagonist). Different B-rings play a major role in distinguishing how and where the ligand binds to AR and whether the pharmacology is a selective AR modulator (SARM) (**9**, **10**), a traditional antiandrogen (**3**), or an SARD (**11**–**13**) with broad-scope AR antagonism, AR degradation, and/or NTD binding.[39,41,42] The latter activity seems to be elicited by basicity-located 5-bond lengths from the A-ring. Based on this hypothesis, here we reported the exploration of the context of the basic nitrogen within a diverse array of monocyclic B-rings. This was accomplished through synthesis and biological evaluation of novel SARDs and pan-antagonists in vitro and in vivo models of CRPC and antiandrogen resistance, including enzalutamide-resistant (EnzR) CRPC tumors.

RESULTS AND DISCUSSION

Chemistry.

Propanamide Derivatives with Heteromonocyclic B-Ring Modifications.—The synthesis of compounds **19a**–**k** is shown in Scheme 1. Commercially available (*R*)-3-bromo-2-hydroxy-2-methylpropanoic acid **14a** was treated with $SOCl_2$ to transform to its acid chloride **14b**, which reacted with aniline **15a** or **15b** in the presence of triethylamine to afford the bromide compound **16a** or **16b**, respectively. Under basic conditions (e.g., K_2CO_3), **16a** was transformed to a key oxirane intermediate **17a**, while **16b** was transformed to oxirane intermediate **17b**. Treatment of **17a** or **17b** with different nucleophiles **18a**–**k** under basic conditions (e.g., sodium hydride) generated propanamides **19a**–**k**, as shown in Scheme 1.

Scheme 2 shows the synthesis of compounds **19l**–**n**. The treatment of commercially available ketone **20a** or **20b** with trimethylsilanecarbonitrile (Me_3SiCN) in the presence of a catalytic amount of zinc iodide (ZnI_2) gave a carbonitrile compound **21a** or **21b**, which was hydrolyzed under hydrogen chloride aqueous conditions to afford the corresponding carboxylic acid **22a** or **22b**, respectively. Compound **22a** or **22b** was treated with $SOCl_2$ to

transform to the acid chloride **23a** or **23b**, which reacted with aniline **24a** or **24b** under basic conditions (e.g., triethylamine) to generate the target compound **19l** or **19m**, respectively. Synthesis of **19n** was achieved by reacting bromine compound **19l** with Cu(I)CN under microwave irradiation, as shown in Scheme 2.

The synthesized propanamides **19a**–**n** initially were tested in vitro for AR LBD binding (K_i), inhibition of transactivation (IC_{50}), and AR degradation (% degradation) of full-length (AR FL in LNCaP cells) and splice variant (AR SV in 22RV1 cells) AR in prostate cancer cell lines. *In vitro* AR inhibition is defined as the ability to inhibit R1881-induced wtAR transcriptional activity as measured by luciferase assay, referred to as in vitro AR inhibition herein. In these studies, we sought to discover novel SARDs and AR pan-antagonists that potently inhibit AR transactivation (IC_{50}), optionally degrade AR FL and AR SV, and possess in vivo efficacy in models of antiandrogen-resistant CRPC of greater potency than **11**–**13**. AR LBD binding (K_i) is helpful in understanding whether these SARDs, which are believed to function via an N-terminal binding site,[38,40] also function at the same site as traditional antiandrogens. Though not prerequisite to screening in vivo, potent LBD binding may help achieve pan-antagonism and thus may be an asset in the treatment of PC, where heavily pretreated patients often have a wide variety of ARs expressed within tumor cells including wtAR, various point mutant ARs, and various truncated ARs, and additionally many have this mix of ARs overexpressed. Accordingly, the broadest possible AR pan-antagonism, including mediated by the LBD, is an asset. Unfortunately, the contribution of LBD vs. NTD binding to IC_{50} is not immediately clear from this in vitro panel. The results are shown in Tables 1 and 2.

We initially explored a series of propanamides with different monocyclic B-rings based on **13** as the initial lead. As shown in Table 1, **19a**, which has a 3-fluoro-1*H*-pyrrol-1-yl moiety as the B-ring, possessed binding affinity with a K_i value of 0.633 μM, while **19b**, which has a 3-cyano-1*H*-pyrrol-1-yl moiety as the B-ring, had increased binding affinity to 0.328 μM, whereas **13** demonstrated no LBD affinity (>10 μM) in this assay. However, both **19a** and **19b** exhibited agonistic activity, which cannot be tolerated in the treatment of PC and no degradation. The unsubstituted imidazol-1-yl **19c** possessed weak AR inhibitory and SARD activity (IC_{50} = 1.856 μM; 0% AR FL and 30% AR SV degradation) vs **13** (IC_{50} = 0.199 μM; 65–100% (FL) and 60–100% (AR SV) AR degradation). Introducing 4-bromine on the imidazole delivered **19d** as a potent partial antagonist (IC_{50} value of 0.14 μM) but no degradation, while 5-bromine on the imidazole gave **19e**, a weak antagonistic activity (IC_{50} = 1.019 μM) but maintained SARD activity (50%/70% AR FL/SV degradation). As such, **19e** was the first pan-antagonist, albeit weak compared to **13**. Similarly, the unsubstituted 1*H*-1,2,4-triazol-1-yl as the B-ring, **19f**, was a weak inhibitor (IC_{50} = 1.091 μM) lacking SARD activity, but its 3-CF_3 analogue **19g** was a pan-antagonist (IC_{50} = 1.013 μM; 68%/100% AR FL/SV degradation) with improved ability to degrade AR relative to **19e**. **19h** with a pyrrolidine as B-ring exhibited no AR inhibitory activity and no protein degradation activity, while **19i** with a morpholine as B-ring again showed pan-antagonism with an IC_{50} value of 1.018 μM and 52 and 80% AR FL and AR SV protein degradation activities, indicating that introduction of the second heteroatom into the ring rescued SARD and LBD binding and overall AR inhibition activity, suggesting that the oxygen atom of the

morpholine B-ring was able to serve the same purpose as electronegative substituents of **19e** and **19g**.

In contrast with **13**, **19j**–**n** in some cases bound the LBD (see **19m** and **19n**) but possessed no inhibitory activity (**19j**) or exhibited AR agonistic activity (**19k**–**n**). Accordingly, linking elements possessing secondary anilines (see **19j** and **19k** (Table 1) vs tertiary anilide **11** (Table 2)) or lacking a basic nitrogen (**19l**–**n**) were not seen as promising features for future structure–activity relationship (SAR) exploration for SARD and pan-antagonist activity. Further, based on this series and previously published SARDs, the basic N-atom seems necessary, but not sufficient (see **19j**–**k**), to confer activity in our screening panel. Further, the biaryl B-ring of **11** or bicyclic B-ring of **12** (Table 2) seems to be beneficial to SARD activities and pan-antagonism.

Propanamide Derivatives with Biaryl or Diaryl B-Ring Modifications.—

Subsequent synthetic modifications were aimed at the replacement of the pyrazole monocyclic B-ring of **13** by a bicyclic B-ring system such as in **11** to explore the effect of the bicyclic system on AR inhibition and SARD activity. The synthesis of **26a**–**e** was performed using similar synthetic methods as in Scheme 1, as depicted in Scheme 3. Treatment of either bromine compound **16a** or oxirane intermediate **17a** with different nucleophiles **25a**–**e** under basic conditions (e.g., sodium hydride) formed propanamides **26a**–**e** (Scheme 3).

Compounds **26f**–**h** were synthesized as shown in Scheme 4. Bromine compound **16a** or **16c** was treated with NaN_3 in DMF to afford azide **27a** or **27b**, respectively. 1,4-Disubstituted-1,2,3-triazole analogues **26f** and **26g** were obtained by copper(I)-catalyzed azide–alkyne cycloaddition (CuAAC) between azide **27a** or **27b** and alkyne **28**, respectively. On the other hand, 1,5-disubstituted-1,2,3-triazole **26h** (regioisomer of **26f**) was prepared by the azide–alkyne Huisgen cycloaddition between azide **27a** and alkyne **28**, as depicted in Scheme 4. The compounds **26a**–**h** were tested in vitro as discussed above for AR activity (Tables 1 and 2).

Temperature.

Given our difficulty in improving AR inhibitory activity via different monocyclic B-rings, we investigated SAR trends for biaryl (**26a**–**d** and **26f**–**h**) and diphenyl (**26e**) B-ring systems (Table 2). The 3-phenyl-1*H*-pyrrol-1-yl B-ring compound **26a** showed AR binding affinity and partial inhibitory activity (K_i = 0.322 μM; IC_{50} = 0.178 μM). Similar to the monocyclic series (Table 1), adding an electronegative substituent tends to improve activity in the screening panel, e.g., introducing a *para*-fluorine to the 3-phenyl-1*H*-pyrrol-1-yl B-ring as in **26b** marginally increased LBD binding affinity (K_i = 0.259 μM) and dramatically increased SARD activity (100% (FL) and 60% (AR SV) degradation) while maintaining potent AR inhibitory activity (IC_{50} value of 0.226 μM). The screening profile of **26b** was comparable to that of **13** with regard to in vitro AR inhibition and SARD activity (0.199 μM; 65–100 and 60–100% AR FL and AR SV degradation), but unlike **13**, **26b** possessed potent LBD binding.

Replacing the pyrrole moiety in **26b** by a pyrazole gave **26c**, which showed weaker AR binding affinity (K_i = 0.612 μM) and weaker inhibitory activity (IC_{50} = 0.969 μM), whereas the tetrazole analogue **26d** possessing 1,5-biaryl arrangement lost AR inhibitory activity.

Diaryl tertiary aniline **26e** with a (4-fluorophenyl)(phenyl)-amino moiety as B-ring exhibited potent LBD binding (K_i = 0.275 μM) and inhibitory activity (IC_{50} = 0.172 μM) but only low to moderate AR degradation (42%/16% FL/SV). Compared to **11**, which bears a methyl group on the basic N-atom, there is substantial steric bulk tolerance around the basic N-atom for LBD binding and AR inhibition, but SARD activity is not maintained, and diphenyl B-rings were not explored further herein.

Compound **26f** possessed a (4-fluorophenyl)-1*H*-1,2,3-triazol-1-yl B-ring and exhibited moderate inhibitory activity (IC_{50} value of 0.383 μM) and moderate-to-high-efficacy degradation (84%/74% FL/SV degradation) but no LBD binding. **26h** is a regioisomer of **26f** that differs from **26f** in the 1,5-biaryl arrangement of the (4-fluorophenyl) and 1,2,3-triazol-1-yl components of the B-ring. **26h** showed inhibitory activity (IC_{50} = 0.317 μM) and FL AR degradation (73% degradation), which was comparable to its regioisomer but improved LBD binding (K_i = 0.703 μM). Contrary to tetrazole **26d**, **26h** suggests tolerance to the 1,5-biaryl arrangement for AR antagonism. Replacing a carbon (CH) with a nitrogen (N) at the 3′-position of the A-ring, i.e., 3′-pyridino derivative of **26f**, delivered a more potent compound (**26g**) with regard to LBD binding (K_i of 1.486 μM vs >10 μM for **26f**) and AR inhibition (IC_{50} value of 0.217 μM vs 0.383 μM for **26f**) but decreased AR degradation activity (12%/0% FL/SV vs 84%/74% FL/SV for **26f**).

Following our discovery of orally bioavailable pyrazole (**13**), we sought to explore the SAR of other basic heteromonocycles as templates for optimization of SARDs and pan-antagonist activities. This survey of B-ring replacements revealed that multiple heteromonocycles preserved FL and SV SARDs together with inhibition of wtAR (LBD binding was optional) fulfilling our definition of pan-antagonist and could serve as a template for further optimization, including pyrroles (**26b**), imidazoles (**19e**), 1,2,4-triazoles (**19g**), morpholino (**19i**), diphenyl aniline (**26e**), and 1,2,3-triazoles (**26f**, **26g**, and **26h**). Lack of an electrophilic substituent on the B-ring moiety (**19c** vs **19e**, **19h** vs **19i**, or **26a** vs **26b**) compromised pan-antagonism, whereas the lack of N-substitution (**19j**–**k**) or lack of basic nitrogen (**19l**–**n**) abrogated pan-antagonism. In some cases, addition of a substituted 4-fluorophenyl ring to the heteromonocycle to produce a biaryl B-ring was tolerated (pyrazole **26c**, 1,2,3-triazoles **26f**–**h**) or improved (pyrrole **26b** vs **19a** or **19b**) pan-antagonist activity in our screening panel. Though not required (see aniline **11** or heterobicycle **12**), having a broad set of active heteromonocycles (in addition to providing broad patent exclusion) affords the advantage of being able to fine-tune biophysical properties such as aqueous solubility and bioavailability and tune out potential liabilities that may emerge during in vivo testing or investigation of new drug (IND)-enabling studies.

In overview, biaryl pyrrole **26b** (K_i > 0.259 μM; IC_{50} = 0.226 μM; 100%/60% FL/SV AR degradation) and biaryl triazole **26f** (K_i > 10 μM like **13**; IC_{50} = 0.383 μM; 84%/74% FL/SV AR degradation) were the only compounds that exhibited potent activity in all aspects of the screening panel. Although **26b** and **26f** had decreased potency LBD binding and AR

inhibition compared to **11** (K_i = 0.078 μM; IC_{50} = 0.048 μM; 70%/71–100% FL/SV AR degradation) and **12** (K_i > 0.267 μM; IC_{50} = 0.085 μM; 65–83%/60–100% FL/SV AR degradation), **11** and **12** suffered from a lack of in vivo activity due to poor bioavailability. However, **26b** and **26f** had comparable inhibitory potency and SARD activity relative to **13** (K_i > 10 μM; IC_{50} = 0.199 μM; 65–100%/60–100% FL/SV AR degradation), which was recently demonstrated to be a bioavailable SARD with exceptional in vivo activities in models of EnzR PC,[38,40] and **26b** has the advantage of potent LBD binding.

Biology.

In Vitro Metabolic Stability in Mouse Liver Microsomes (MLMs).—Selected compounds **19c**, **19e**, **26a**, **26b**, **26e**, **26f**, and **26h** were evaluated for in vitro metabolic stability in mouse liver microsomes (MLMs) with cofactors for enzymes of both phase I and phase II metabolism. The half-life ($T_{1/2}$) and intrinsic clearance (CL_{int}) values were calculated as a predictor of the distribution, metabolism, and pharmacokinetic (DMPK) properties of these compounds (Table 3). The CL_{int} of these compounds **19c**, **19e**, **26b, 26f**, and **26h** was slower than previously published SARDs **11** ($T_{1/2}$ of 1.15 min) and **12** ($T_{1/2}$ of 12.11 min); especially compounds **26f** and **26h** were even slower than **13**, which was orally bioavailable ($T_{1/2}$ of 78 min),[40] producing relatively stable $T_{1/2}$ values of 265 min and >360 min in MLM, respectively. Compound **26a**, which has a 3-phenyl-1*H*-pyrrol-1-yl B-ring, and **26e** (diphenyl aniline) showed relatively unfavorable in vitro metabolic stability with $T_{1/2}$ values of 3.96 and 5.07 min, as well as CL_{int} values of 157.5 and 136.8 mL/min/mg, respectively. **26b**, in which *para*-fluorine is introduced on the 3-phenyl-1*H*-pyrrol-1-yl B-ring, increased $T_{1/2}$ by ~4-fold to 17.93 min, suggesting that the fluorination protected the phenyl ring from metabolism. Compounds **26f** and **26h**, both of which have a 1,2,3-triazole B-ring, dramatically increased $T_{1/2}$, suggesting that the triazole moiety had a very favorable in vitro metabolic stability. This was a significant improvement when compared to previous SARD templates with a bicyclic B-ring such as 1.15 min for the tertiary amine **11** and 12.11 min for lead indole **12**.[38,39] This supports that compound **26f** may be stable enough in liver metabolism to attain optimum to high blood levels upon oral administration and be distributed to sites of action throughout the body, as would be necessary to treat CRPC. Further, **26f** compares favorably to other compounds reported herein with regard to inhibitory potency and SARD efficacy (Tables 1 and 2). Correspondingly, **26f** was advanced to testing in models of CRPC including resistance to **5** (EnzR MR49F cells harboring F876L and T877A AR point mutations) and **3** (bicalutamide-resistant LNCaP cells harboring the T877A mutation).

Androgen Receptor Target Gene Expression in CRPC Cells.—To evaluate whether the observed highly potent AR antagonism translates to inhibition of endogenous AR function, we performed an AR target gene inhibitory experiment to determine the effect of **26f** in LNCaP cells and compared it with enzalutamide (**5**) (Figure 3). **26f** was chosen as the lead compound because **26f** possessed a balance of high potency inhibition (0.383 μM), high-efficacy degradation (84% for AR FL and 74% AR SV), and long in vitro stability ($T_{1/2}$ of 265 min) compared to other SARDs and pan-antagonists screened. Consistent with the 0.383 μM inhibition of wtAR transactivation, *FKBP5* gene expression induced by 0.1 nM R1881 induced in LNCaP cells was robustly inhibited by **26f** at concentrations as low as

1 μM (Figure 3A), which was similar to **5**, and 0.1 nM R1881-induced *PSA* gene expression in LNCaP cells was inhibited by **26f** at concentrations 10 μM as potent as **5** (Figure 3B).

Concurrently, we tested the effect of **26f** on the function of **5** resistance-conferring F876L/T877A AR in the context of LNCaP cells, i.e., MR49F cells. Similarly, dose-dependent downregulation of *FKBP5* gene expression was seen in MR49F cells when treated with **26f** but not **5**, validating this as a model of EnzR. 26f inhibited the expression of *FKBP5* at concentrations as low as 0.3 μM in EnzR LNCaP (Figure 3C), indicating that the clinically significant F876L mutant was potently sensitive to **26f**. Cumulatively, the data above support that **26f** has pan-antagonist effects in at least wtAR (IC_{50} value in Table 2), T877A (AR FL degradation in Table 2), F876L/T877A (Figure 3C; see also degradation in MR49F cells, as reported *infra*), and AR SV (degradation in Table 2).

Proliferation Studies in PC Cells.—To determine whether the potent functional inhibition and degradation of AR translate into the inhibition of PC cell growth, the effect of **26f** was tested in an LNCaP cell model of CRPC harboring the T877A antiandrogen resistance mutation and in an even more refractory model of CRPC, i.e., MR49F cells. In the absence of an AR antagonist, R1881 induced proliferation of androgen-dependent LNCaP cells (not shown). Antiproliferative effects were tested in the presence of a titrated dose of **26f** or **5**, as shown in Figure 4A. **26f** demonstrated antiproliferation at doses as low as 10 μM and full efficacy at 30 μM, while **5** exhibited little effect on the proliferation in LNCaP cells (Figure 4A). A modest inhibition of proliferation in the presence of **26f**, but not **5**, was observed in AR-negative PC3 cells (Figure 4B) consistent with AR-dependent antiproliferation. As mentioned above, the F876L mutation confers EnzR to MR49F cells; however, MR49F cells remain dependent on the AR for growth. R1881-induced MR49F proliferation was inhibited by **26f** in the 10 μM and full efficacy at 30 μM (Figure 4C) similar to the parental LNCaP (Figure 4A), whereas **5** showed no effect of the proliferation in the MR49F model (Figure 4C). Assuming that **26f** can reach the tumors and androgen-dependent organs in sufficient concentrations, this potent antiproliferation of **26f** suggests that **26f** may perform well in in vivo models.

AR FL (F876L) and AR SV (AR-V7) Degradation in Models of CRPC.—To ensure that the in vitro AR antagonism profiles of **26f** were also maintained in an EnzR cell line, FL AR degradation studies in MR49F cells were performed. Figure 5 shows that **26f**, but not **5**, degraded this mutant FL AR in MR49F cells, i.e., a model of EnzR CRPC, in a dose-responsive manner (top panel), consistent with the ability of **26f** to degrade AR in LNCaP (Table 2) and suppress AR-dependent gene expression in LNCaP and MR49F cells (Figure 3). The Western blots were quantified densitometrically, and the AR/GADPH values are represented as percent change from vehicle-treated cells.

High-efficacy SARD activity was observed with **26f** at 1 μM and complete degradation at 10 μM (Figure 5, top panel), indicating that this mutant AR FL that confers EnzR in MR49F LNCaP cells is susceptible to destruction by **26f**.

The middle panel demonstrated that **26f** did not just induce degradation of AR FL in EnzR LNCaP (MR49F cells; Figure 5, top panel) and LNCaP (Table 2) but can also degrade AR

SVs such as the AR-V7 (22RV1 cells; lower band of the middle panel of Figure 5). As reported in Table 2 (see the AR SV degradation column), **26f** was able to reduce AR-V7 levels by 74% in 22RV1 cells at 10 μM. PCs expressing AR SVs possess no binding site for traditional (or canonical) antiandrogens to bind AR, are associated with poor prognosis, and are believed to be resistant to approved therapies including **2**–**7**.[44] Taken together, **26f** affords a very broad scope of AR antagonistic abilities.

In Vivo Models.

Preliminary Pharmacokinetic (PK) Study with 26f in Mice.—C57BL/6 mice (n = 4/time point) were treated with a single dose of 30 mg/kg orally of **26f**. Blood was collected 6 and 24 h after dosing, and serum **26f** concentration was measured. The average serum concentrations of **26f** at 6 and 24 h after dosing were 453 and 332 nM, respectively. These results suggested that **26f** maintains serum concentrations above to around the AR inhibitory IC_{50} value of 0.383 μM for greater than 24 h after dosing. This PK behavior is consistent with promising in vivo data such as Hershberger and xenograft studies following oral administration, as reported hereinbelow.

Hershberger Assays in Rats.—Given the metabolic stability in vitro ($T_{1/2}$ of 265 min) and in preliminary PK observations in vivo, we were hopeful that the in vitro SARD and pan-antagonist activity of **26f** would translate into clinically meaningful efficacy in vivo. As expected, Hershberger assays on **26f** orally administered in intact rats demonstrated atrophy of AR-dependent seminal vesicle tissues (Figure 6). Previously, we demonstrated that **13** (4-F pyrazole; IC_{50} of 0.199 μM; $T_{1/2}$ of 78 min) was able to reduce the ventral prostate weight by ~70% at 60 mg/kg po [see Figure S4C, middle panel in Ponnusamy et al.] versus ~40% for 30 mg/kg po of **5**, both in rats. At 20 mg/kg po of **26f**, that is, one-third of the dose of **13** mentioned above, seminal vesicle weights were reduced by 49% (Figure 6), demonstrating that the in vivo pharmacodynamic properties intrinsic to **26f** are observable at lower doses relative to **13**. Compared to **13**, introducing of the 4-(4-fluorophenyl)-1*H*-1,2,3-triazol-1-yl moiety as the B-ring seemed favorable for metabolic stability and in vivo antagonism, suggesting that xenograft potencies should also be improved. These results confirm that the oral pharmacokinetics of **26f** was sufficiently robust to allow **26f** to be absorbed and distributed to the site of action in AR target organs and suggested that **26f** should also distribute to tumors in xenograft models and exert antitumor effects in sensitive models.

EnzR (MR49F) LNCaP Xenografts in Mice.—The PC studies described above were in vitro models that provided support that **26f** inhibited and degraded both AR FL and truncation mutant AR (AR SV), as well as in vivo antagonism in Hershberger assays with 49% change in seminal vesicle weights relative to intact vehicle control. To evaluate the effect of **26f** in an enzalutamide-resistant xenograft model, EnzR LNCaP (MR49F) cells were implanted subcutaneously in NOD SCID γ (NSG) mice. Once tumor sizes reached 200–400 mm^3, the mice were castrated, and the tumors were allowed to regrow as CRPC. The animals were treated with vehicle (poly(ethylene glycol)-300/DMSO 85:15 ratio) or 60 mg/kg **26f**, and the tumor volume was measured twice weekly for 28 d. In Figure 7, **26f** significantly reduced the tumor volume with an over 95% tumor growth inhibition (TGI, p

< 0.05; see the last four time points), whereas **5** failed to reduce the tumor volume of EnzR LNCaP xenografts (enzalutamide data not shown here; see Figure 7B in Hwang et al.[39]).

Further, the significant levels of TGI activity indicated that **26f** is orally bioavailable (unlike **11** and **12**) and can reach adequate levels in tumors to reveal the pharmacodynamic behavior of our SARDs, albeit at high dose. The susceptibility of these EnzR xenografts to **26f** in this experiment provides evidence that a triazole SARD, e.g., **26f**, can overcome EnzR CRPC in vivo. Moreover, no loss in body weight was observed in animals treated with **26f** for 14 or 28 d (Hershberger or xenograft, respectively). This indicates that **26f** was not toxic at least at the efficacy doses. Extensive toxicity evaluation needs to be conducted at a concentration that are 5–10 times higher than the efficacy doses. In overview, these experiments provide hope that our SARDs with their unique biological profile could be used to overcome EnzR in CRPC patients.

CONCLUSIONS

Compounds **26b**, **26e**, **26f**, **26g**, and **26h** from the biaryl B-ring series exhibited potent nM range inhibitory activity in vitro. Compounds **19e**, **19g**, and **19i** from the monocyclic B-ring series possessed moderate-to-high SARD efficacy but inhibitory activity of only ~1 μM, whereas biaryls **26b**, **26c**, **26f**, and **26h** similarly possessed moderate-to-high-efficacy SARD activity but nM level in vitro inhibition, as shown in Tables 1 and 2. **19c**, **19e**, **26b**, **26f**, and **26h** improved their DMPK properties in mouse liver microsomes (MLMs) compared to previous SARD templates such as for the tertiary amine **11** ($T_{1/2}$ of 1.15 min) and lead indole **12** ($T_{1/2}$ of 12.11 min); especially, DMPK properties in MLM of **26f** ($T_{1/2}$ of 265 min) and **26h** ($T_{1/2}$ of >360 min), which were even better than that of pyrazole **13** ($T_{1/2}$ of 77.96 min). The lead compound **26f** effectively inhibited the expression of *FKBP5* and *PSA* (Figure 3), as well as demonstrated a dose-responsive antiproliferation in androgen-dependent LNCaP and EnzR LNCaP CRPC cells, but only weakly inhibited androgen-independent PC3 PC cells (Figure 4). Further, SARD activity was maintained in the EnzR CRPC setting (Figure 5), all supporting testing of **26f** in vivo. Compound **26f** produced AR antagonism in an intact rat Hershberger assay, with an approximately 49% reduction in the seminal vesicle weight compared to their intact organ weights (Figure 6). EnzR LNCaP (MR49F) xenograft experiments with 60 mg/kg po daily of **26f** produced significant efficacy of up to 95% TGI (Figure 7). Accordingly, biaryl SARDs such as 4-fluorophenyl-1,2,3-triazole **26f** may have some advantages over pyrazoles such as **13** and are believed to hold great potential for overcoming enzalutamide resistance in CPRC, which is increasingly prevalent in the clinic.

EXPERIMENTAL SECTION

Chemistry.

General Procedures, Materials, and Information.—All solvents and chemicals were used as purchased without further purification. The progress of all reactions was monitored by the thin-layer chromatography (TLC) analysis on silica gel 60 F254 plates (Merck). Column chromatography was performed with a silica gel column (Merck Kieselgel 60, 70–230 mesh, Merck). All nonaqueous reactions were performed in oven-dried glassware under

an inert atmosphere of dry nitrogen. All of the reagents and solvents were purchased from Sigma-Aldrich (St. Louis, MO), Alfa-Aesar (Ward Hill, MA), Combi-Blocks (San Diego, CA), and Ark Pharm (Libertyville, IL) and used without further purification. Analytical thin-layer chromatography was performed on Silica Gel GHLF 10 × 20 cm^2 Analtech TLC Uniplates (Analtech, Newark, DE) and was visualized by fluorescence quenching under UV light. The Biotage SP1 flash chromatography purification system (Charlotte, NC) (Biotage SNAP Cartridge, silica, 50 and 100 g) was used to purify the compounds. ^{1}H NMR and ^{13}C NMR spectra were recorded on a Bruker Ascend 400 (400 MHz) (Billerica, MA) spectrometer. Chemical shifts for ^{1}H NMR were reported in parts per million (ppm) downfield from tetramethylsilane (δ) as the internal standard in deuterated solvent, and coupling constants (J) are in hertz (Hz). The following abbreviations are used for spin multiplicity: s = singlet, d = doublet, t = triplet, q = quartet, quin = quintet, dd = doublet of doublets, dt = doublet of triplets, qd = quartet of doublets, dquin = doublet of quintets, m = multiplet, and br s = broad singlet. Low-resolution mass spectra (MS) were acquired using a Bruker ESQUIRE electrospray/ion trap instrument in the positive and negative modes. High-resolution mass spectrometer (HRMS) data were acquired on a Waters Xevo G2-S QTOF (Milford, MA) system equipped with an Acquity I-class UPLC system. The purity of the final compounds was analyzed by an Agilent 1100 HPLC system (Santa Clara, CA). High-performance liquid chromatography (HPLC) conditions: 45% acetonitrile at a flow rate of 1.0 mL/min using a Luna 5 μm C18 100A column (250 × 4.60 mm^2) purchased from Phenomenex (Torrance, CA) at an ambient temperature. UV detection was set at 340 or 245 nm. Purities of the compounds were established by careful integration of areas for all peaks detected and determined as ≥95% for all compounds tested for the biological study.

General Procedure A for the Synthesis of 16a–c Using (R)-3-Bromo-N-(4-cyano-3-(trifluoromethyl)phenyl)-2-hydroxy-2-methylpropanamide (16a) as an Example.—(*R*)-3-Bromo-2-hydroxy-2-methylpropanoic acid **14a** (5.00 g, 27 mmol) was dissolved in THF (27 mL, 5.4 vol) in an EasyMax 100 mL reactor. Agitation was set to 400 rpm, and the solution was cooled to 2.5 °C. Thionyl chloride (2.39 mL, 1.20 equiv, 0.48 vol) was slowly added to the reaction mixture over 30 min while maintaining the reaction temperature below 12 °C. The reaction mixture was stirred for 1.5 h. The reaction was cooled to −5 °C. Triethylamine (5.0 mL, 1.30 equiv, 1 vol) was slowly added to the reaction mixture, keeping the temperature below 12 °C. 4-Amino-2-(trifluoromethyl)benzonitrile **15a** (4.85 g, 0.95 equiv, 0.97 wt) and THF (3.37 mL, 0.67 vol) were then charged to the batch. The batch was then heated to 50 ± 5 °C and agitated for 2 h. The batch was then cooled to 20 ± 5 °C followed by the addition of water (14.7 mL, 2.9 vol) and toluene (20.2 mL, 4.0 vol). After brief agitation, the layers were separated. The organic layer was then washed with water (14.7 mL, 2.9 vol). The batch was then concentrated to 5 ± 0.5 volumes (4 ± 0.5 wt) while maintaining the batch temperature below 50 °C, followed by the addition of toluene (30 mL, 6 vol). The batch was then distilled to 5 ± 0.5 volumes (4 ± 0.5 wt), and the batch temperature was reduced to 2.5 ± 2.5 °C. The batch was then filtered, and the filter cake was washed with toluene twice (8.5 mL each, 1.7 vol each). The batch was then dried under 25–30 in. vacuum to provide **16a**.

General Procedure B for the Synthesis of 17a and 17b Using (S)-N-(4-Cyano-3-(trifluoromethyl)phenyl)-2-methyloxirane-2-carbox-amide (17a) as an Example.—To a solution of (*R*)-3-bromo-*N*-(4-cyano-3-(trifluoromethyl)phenyl)-2-hydroxy-2-methylpropanamide (**16a**) (5.00 g, 0.018504 mol) in 25 mL of 2-butanone was added potassium carbonate (3.836 g, 0.027756 mol). The resulting reaction mixture was heated at reflux for 2 h under an argon atmosphere. After the end of the reaction was established by TLC, the reaction was cooled to room temperature (rt), filtered through a pad of celite, and the celite pad was rinsed with 15 mL of 2-butanone. The filtrate was concentrated under vacuum and dried under 25–30 in. vacuum to provide **17a**.

General Procedure C for the Synthesis of 19a–k and 26a–e Using 19b as an Example (Schemes 1 and 3).—To a solution of 1*H*-pyrrole-3-carbonitrile (0.10 g, 0.00108 mol) in anhydrous THF (10 mL), which was cooled in an ice–water bath under an argon atmosphere, was added sodium hydride (60% dispersion in oil, 0.09 g, 0.00217 mol). After addition, the resulting mixture was stirred for 3 h. (*R*)-3-Bromo-*N*-(4-cyano-3-(trifluoromethyl)phenyl)-2-hydroxy-2-methylpropanamide (**16a**) (0.38 g, 0.00108 mol) was added to the above solution, and the resulting reaction mixture was allowed to stir overnight at rt under argon. The reaction was quenched with water and extracted with ethyl acetate. The organic layer was washed with brine, dried with $MgSO_4$, filtered, and concentrated under vacuum. The product was purified by a silica gel column using ethyl acetate and hexanes (1:1) as eluent to afford 0.26 g of **19b** as a white solid.

General Procedure D for the Synthesis of 19l and 19m Using 19l as an Example (Scheme 2).—The trimethylsilanecarbonitrile (Me_3SiCN) (2 equiv) was added to a solution of ketone (**20a**) (1 equiv) and a catalytic amount of zinc iodide (ZnI_2) in dichloro-methane. The resulting reaction mixture was stirred at rt overnight. After the end of reaction was established by TLC, the solvents were evaporated under vacuum to afford crude **21a**. Twenty milliliters of concentrated HCl and 5 mL of ethyl acetate were added to the residue of tertiary alcohol **21a**, and the mixture was stirred for 1 h. The mixture was cooled to rt, and ice-cold 1 N NaOH was added slowly to dissolve the solid. The mixture was extracted with dichloromethane three times. To the water layer, concentrated HCl was added and extracted with dichloromethane, the combined dichloromethane was dried over anhydrous sodium sulfate, and the solvents were evaporated. The white solid was purified by redissolving in NaOH, filtered and acidified with 1 N HCl, and extracted with ethyl acetate. The organic layer was dried over sodium sulfate and evaporated to get acid **22a**. The corresponding acid **22a** was taken in dry THF, cooled to 0 °C, and thionyl chloride (1.5 equiv) was added and stirred for 90 min. To the mixture, triethylamine (5 equiv) and corresponding aniline **24a** (1 equiv) were added and refluxed overnight. The reaction was cooled to rt and extracted with ethyl acetate. The organic layer was dried and evaporated and subjected to flash chromatography to afford **19l**.

(*S*)-*N*-(4-Cyano-3-(trifluoromethyl)phenyl)-3-(3-fluoro-1*H*-pyrrol-1-yl)-2-hydroxy-2-methylpropanamide (19a).: Compound **19a** was prepared following General Procedure C per Scheme 1. The product was purified by a silica gel column using ethyl acetate and hexanes (1:1) as eluents to afford 0.181 g of the titled

compound as a white solid. Yield = 31%. ^{1}H NMR (400 MHz, $CDCl_3$) δ: 8.91 (bs, 1H, NH), 8.03 (d, J = 2.0 Hz, 1H), 7.90 (dd, J = 8.4, 2.0 Hz, 1H), 7.81 (d, J = 8.4 Hz, 1H), 6.47 (m, 1H), 6.41 (m, 1H), 5.91 (dd, J = 2.8, 2.0 Hz, 1H), 4.36 (d, J = 14.4 Hz, 1H), 3.98 (d, J = 14.4 Hz, 1H), 1.54 (s, 3H). ^{19}F NMR ($CDCl_3$, decoupling) δ −62.18, −164.26. HRMS [$C_{16}H_{14}F_4N_3O_2^+$]: calcd 356.1022, found 356.1021 [M + H]$^+$.

(*S*)-3-(3-Cyano-1*H*-pyrrol-1-yl)-*N*-(4-cyano-3-(trifluoromethyl)phenyl)-2-hydroxy-2-methylpropanamide (19b).: Compound **19b** was prepared following General Procedure C per Scheme 1. The product was purified by a silica gel column using ethyl acetate and hexanes (1:1) as eluents to afford 0.26 g of the titled compound as a pinkish solid. Yield = 51.3%. ^{1}H NMR (400 MHz, DMSO-d_6) δ: 10.44 (s, 1H, NH), 8.44 (s, 1H, ArH), 8.24 (d, J = 8.8 Hz, 1H, ArH), 8.10 (d, J = 8.8 Hz, 1H, ArH), 7.49 (s, 1H, pyrrole-H), 6.38 (t, J = 2.0 Hz, 1H, pyrrole-H), 6.41–6.40 (m, 2H, OH and pyrrole-H), 4.30 (d, J = 14.0 Hz, 1H, CH), 4.14 (d, J = 14.0 Hz, 1H, CH), 1.34 (s, 3H, CH_3). HRMS [$C_{17}H_{14}F_3N_4O_2^+$]: calcd 363.1069, found 363.1079 [M + H]$^+$. Analytical HPLC showed a 97.92% purity.

(*S*)-*N*-(3-Chloro-4-cyanophenyl)-2-hydroxy-3-(1*H*-imidazol-1-yl)-2-methylpropanamide (19c).: Compound **19c** was prepared following General Procedure C per Scheme 1. Under an argon atmosphere, a 2.0 M lithium diisopropylamide solution (1.25 mL, 2.5 mmol) in THF/heptane/ethylbenzene was slowly added in a dropwise manner over 10 min to a solution of imidazole (68 mg, 1.0 mmol) in 5 mL of anhydrous THF at −78 °C and warmed to 0 °C and stirred for 10 min and cooled again to −78 °C. To the solution was added in a dropwise fashion a solution of bromide (315 mg, 1.0 mmol), and the reaction mixture was stirred overnight. After quenching by the addition of sat. NH_4Cl, the solution was concentrated under reduced pressure and dispersed into excess EtOAc and dried over Na_2SO_4. The product was purified by a silica gel column using ethyl acetate and hexanes (2:1) as eluents to afford the titled compound as a white solid. Yield = 65%. ^{1}H NMR (400 MHz, $CDCl_3$) δ: 10.24 (bs, 1H, NH), 8.19 (s, 1H), 7.90 (s, 2H), 7.53 (s, 1H), 7.05 (s, 1H), 6.82 (s, 1H), 6.40 (s, 1H), 4.30 (d, J = 14.4 Hz, 1H), 4.13 (d, J = 14.4 Hz, 1H), 3.34 (bs, 1H, OH), 1.34 (s, 3H). HRMS [$C_{14}H_{14}ClN_4O_2^+$]: calcd 305.0805, found 305.0854 [M + H]$^+$. Analytical HPLC showed a 99.75% purity.

(*S*)-3-(4-Bromo-1*H*-imidazol-1-yl)-*N*-(4-cyano-3-(trifluoromethyl)phenyl)-2-hydroxy-2-methylpropanamide (19d).: Compound **19d** was prepared following General Procedure C per Scheme 1. The product was purified by a silica gel column using DCM and methanol (19:1) as eluents to afford the titled compound as a white solid. Yield = 32%. ^{1}H NMR (400 MHz, $CDCl_3$) δ: 9.48 (bs, 1H, NH), 8.15 (s, 1H), 7.97 (d, J = 8.6 Hz, 1H), 7.83 (d, J = 8.6 Hz, 1H), 7.71 (s, 1H), 6.75 (s, 1H), 4.53 (d, J = 14.4 Hz, 1H), 4.09 (d, J = 14.4 Hz, 1H), 2.84 (s, 1H, OH), 1.45 (s, 3H). ^{19}F NMR (400 MHz, $CDCl_3$) δ −62.19. HRMS [$C_{15}H_{13}BrF_3N_4O_2^+$]: calcd 417.0174, found 417.0174 [M + H]$^+$. Analytical HPLC showed a 98.33% purity.

(*S*)-3-(5-Bromo-1*H*-imidazol-1-yl)-*N*-(4-cyano-3-(trifluoromethyl)phenyl)-2-hydroxy-2-methylpropanamide (19e).: Compound **19e** was prepared following General Procedure C per Scheme 1. The product was purified by a silica gel column using ethyl acetate and

hexanes (1:1) as eluents to afford the titled compound as a white solid. Yield = 37%. ^{1}H NMR (400 MHz, acetone-d_6) δ: 9.93 (bs, 1H, NH), 8.44 (d, J = 2.0 Hz, 1H), 8.26 (dd, J = 8.6, 2.0 Hz, 1H), 8.03 (d, J = 8.6 Hz, 1H), 7.47 (s, 1H), 7.11 (s, 1H), 5.83 (s, 1H, OH), 4.50 (d, J = 14.0 Hz, 1H), 4.23 (d, J = 14.0 Hz, 1H), 1.55 (s, 3H). ^{19}F NMR (400 MHz, acetone-d_6) δ 114.69. HRMS [$C_{15}H_{13}BrF_3N_4O_2^+$]: calcd 417.0174, found 417.0175 [M + H]$^+$. Analytical HPLC showed a 95.15% purity.

(*S*)-*N*-(4-Cyano-3-(trifluoromethyl)phenyl)-2-hydroxy-2-methyl-3-(1*H*-1,2,4-triazol-1-yl)propanamide (19f).: Compound **19f** was prepared following General Procedure C per Scheme 1. The product was purified by a silica gel column using ethyl acetate and hexanes (2:3) as eluent to afford 0.143 g of the titled compound as white solid. Yield = 43%. ^{1}H NMR (400 MHz, $CDCl_3$) δ: 9.10 (bs, 1H, NH), 8.15 (s, 1H), 8.02 (d, J = 2.0 Hz, 1H), 7.88 (dd, J = 8.4, 2.0 Hz, 1H), 7.78 (d, J = 8.4 Hz, 1H), 5.70 (bs, 1H, OH), 4.79 (d, J = 14.0 Hz, 1H), 4.35 (d, J = 14.0 Hz, 1H), 1.53 (s, 3H). ^{19}F NMR (400 MHz, $CDCl_3$, decoupling) δ −62.22. HRMS [$C_{14}H_{13}F_3N_5O_2^+$]: calcd 340.1021, found 340.1026 [M + H]$^+$. Analytical HPLC showed 99.53% purity.

(*S*)-*N*-(4-Cyano-3-(trifluoromethyl)phenyl)-2-hydroxy-2-methyl-3-(3-(trifluoromethyl)-1*H*-1,2,4-triazol-1-yl)-propanamide (19g).: Compound **19g** was prepared following General Procedure C per Scheme 1. The product was purified by a silica gel column using ethyl acetate and hexanes (2:3) as eluents to afford 0.213 g of the titled compound as a white solid. Yield = 53%. ^{1}H NMR (400 MHz, acetone-d_6) δ: 9.88 (bs, 1H, NH), 9.44 (s, 1H), 8.44 (s, 1H), 8.25 (d, J = 8.4 Hz, 1H), 8.04 (d, J = 8.4 Hz, 1H), 4.82 (d, J = 14.4 Hz, 1H), 4.61 (d, J = 14.4 Hz, 1H), 2.88 (bs, 1H, OH), 1.61 (s, 3H). ^{19}F NMR (400 MHz, $CDCl_3$) δ −62.26, −65.25. HRMS [$C_{15}H_{12}F_6N_5O_2^+$]: calcd 408.0895, found 408.0898 [M + H]$^+$. Analytical HPLC showed a 98.52% purity.

(*S*)-*N*-(3-Chloro-4-cyanophenyl)-2-hydroxy-2-methyl-3-(pyrrolidin-1-yl)propanamide (19h).: Compound **19h** was prepared following General Procedure C per Scheme 1. The product was purified by a silica gel column using ethyl acetate and hexanes (1:2) as eluents to afford 0.277 g of the titled compound as a colorless oil. Yield = 90%. ^{1}H NMR (400 MHz, $CDCl_3$) δ: 9.41 (bs, 1H, N*H*), 7.98 (d, J = 2.0 Hz, 1H), 7.62 (d, J = 8.8 Hz, 1H), 7.51 (dd, J = 8.8, 2.0 Hz, 1H), 3.15 (d, J = 12.4 Hz, 1H), 2.72 (d, J = 12.4 Hz, 1H), 2.62 (m, 4H), 1.76 (m, 4H), 1.52 (s, 1H, O*H*), 1.41 (s, 3H). HRMS [$C_{15}H_{19}ClN_3O_2^+$]: calcd 308.1166, found 308.1173 [M + H]$^+$. Analytical HPLC showed a 98.98% purity.

(*S*)-*N*-(4-Cyano-3-(trifluoromethyl)phenyl)-2-hydroxy-2-methyl-3-morpholinopropanamide (19i).: Compound **19i** was prepared following General Procedure C per Scheme 1. The product was purified by a silica gel column using ethyl acetate and hexanes (1:2) as eluents to afford 0.209 g of the titled compound as a white solid. Yield = 88%. ^{1}H NMR (400 MHz, $CDCl_3$) δ: 9.36 (bs, 1H, NH), 8.08 (d, J = 1.6 Hz, 1H), 7.94 (dd, J = 8.4, 1.6 Hz, 1H), 7.80 (d, J = 8.4 Hz, 1H), 3.68 (m, 4H), 3.28 (d, J = 13.2 Hz, 1H), 2.55 (m, 4H), 2.42 (d, J = 13.2 Hz, 1H), 1.50 (bs, 1H, OH), 1.42 (s, 3H). ^{19}F NMR (400 MHz, acetone-d_6) δ −62.20. HRMS [$C_{16}H_{19}F_3N_3O_2^+$]: calcd 358.1379, found 358.1383 [M + H]$^+$. Analytical HPLC showed a 97.38% purity.

(*S*)-3-((1*H*-1,2,4-Triazol-3-yl)amino)-*N*-(4-cyano-3-(trifluoromethyl)phenyl)-2-hydroxy-2-methylpropanamide (19j).: Compound **19j** was prepared following General Procedure C per Scheme 1. The product was purified by a silica gel column using DCM and methanol (19:1) as eluents to afford the titled compound as a brown solid. Yield = 45%. ^{1}H NMR (400 MHz, $CDCl_3$) δ: 9.10 (bs, 1H, N*H*), 8.01 (bs, 1H, N*H*), 8.14 (s, 1H), 7.88–7.76 (m, 2H), 7.72 (s, 0.57H), 7.51 (bs, N*H*, 0.43H), 5.90 (bs, N*H*, 0.57H), 4.74 (bs, OH, 0.43H), 4.55 (d, J = 14.4 Hz, 0.43H), 4.54 (d, J = 13.6 Hz, 0.57H), 4.24 (bs, OH, 0.57H), 4.07 (d, J = 13.6 Hz, 0.57H), 3.97 (d, J = 14.4 Hz, 0.43H), 1.56 (s, 1.29H), 1.48 (s, 1.71H). HRMS [$C_{14}H_{14}F_3N_6O_2^+$]: calcd 355.1130, found 355.1133 $[M + H]^+$. Analytical HPLC showed a 92.43% purity.

(*S*)-*N*-(4-Cyano-3-(trifluoromethyl)phenyl)-3-((4-cyano-3-(trifluoromethyl)phenyl)amino)-2-hydroxy-2-methylpropanamide (19k).: Compound **19k** was prepared following General Procedure C per Scheme 1. The product was purified by a silica gel column using DCM and methanol (19:1) as eluents to afford the titled compound as a yellowish solid. Yield = 9%. ^{1}H NMR (400 MHz, DMSO-d_6) δ: 10.46 (s, 1H, NH), 8.46 (d, J = 2.0 Hz, 1H, ArH), 8.21 (dd, J = 8.2 Hz, J = 2.0 Hz, 1H, ArH), 8.08 (d, J = 8.2 Hz, 1H, ArH), 7.19–7.15 (m, 2H), 6.98 (dd, J = 8.8 Hz, J = 2.4 Hz, 1H, ArH), 6.17 (s, 1H, OH), 3.65–3.60 (m, 1H, CH), 3.38–3.34 (m, 1H, CH), 1.43 (s, 3H, CH_3). MS (ESI) m/z 457.05. $[M + H]^+$. HRMS [$C_{20}H_{15}F_6N_4O_2^+$]: calcd 457.1099, found 457.1100 $[M + H]^+$. Analytical HPLC showed a 97.37% purity.

***N*-(4-Nitro-3-(trifluoromethyl)phenyl)-4-(4-fluorophenyl)-2-hydroxy-2-methylbutanamide (19l).:** Compound **19l** was prepared following General Procedure D per Scheme 2. The product was purified by a silica gel column using DCM and methanol (19:1) as eluents to afford the titled compound as a brown solid. Yield = 43%. HRMS [$C_{18}H_{19}F_3N_3O_4^+$]: calcd 398.1328, found 398.1331 $[M + H]^+$.

4-(4-Bromophenyl)-2-hydroxy-2-methyl-*N*-(4-cyano-3-(trifluoromethyl)phenyl)butanamide (19m).: Compound **19m** was prepared following General Procedure D per Scheme 2. The product was purified by a silica gel column using DCM and methanol (19:1) as eluents to afford the titled compound as a white brown solid. Yield = 45%. ^{1}H NMR (400 MHz, $CDCl_3$) δ: 9.14 (s, 1H, NH), 8.09 (s, 1H, ArH), 7.91 (d, J = 8.4 Hz, 1H, ArH), 7.77 (d, J = 8.4 Hz, 1H, ArH), 7.33 (d, J = 8.4 Hz, 2H, ArH), 7.04 (d, J = 8.4 Hz, 2H, ArH), 2.74–2.81 (m, 1H, CH), 2.52–2.59 (m, 1H, CH), 2.28–2.36 (m, 1H, CH), 1.90–1.97 (m, 1H, CH), 1.58 (s, 3H, CH_3); ^{13}C NMR ($CDCl_3$) δ 27.32, 29.52, 41.86, 76.65, 104.43, 115.54, 117.14, 120.75, 121.68, 130.13, 131.57, 133.92, 135.06, 139.73, 141.49, 173.88. MS (ESI): m/z 440.8 $[M – H]^-$.

***N*-(4-Cyano-3-(trifluoromethyl)phenyl)-4-(4-cyanophenyl)-2-hydroxy-2-methylbutanamide (19n).:** Compound **19n** (1 equiv) and Cu(I)CN (10 equiv) were dissolved in 2 mL of dry dimethylformamide and subjected to microwave irradiation (80 W) at 150 °C for 1 h. After irradiation, the mixture was cooled to rt. The mixture was extracted with ethyl acetate, the organic layer was washed with brine and water, and dried over anhydrous

sodium sulfate. Evaporation of the solvent afforded the titled compound as a yellowish solid. Yield = 32%. ^{1}H NMR (400 MHz, $CDCl_3$) δ: 7.53–7.58 (m, 3H, ArH & NH), 7.29 (d, J = 8.0 Hz, 2H, ArH), 6.95 (s, 1H, ArH), 6.78 (d, J = 8.4 Hz, 2H, ArH), 4.46 (br. S, 1H, OH), 2.95 (t, J = 7.6 Hz, 2H, CH_2), 2.79 (t, J = 7.6 Hz, 2H, CH_2), 2.14 (s, 3H, CH_3); ^{13}C NMR (400 MHz, $CDCl_3$) δ 26.87, 29.16, 41.86, 75.92, 104.11, 109.82, 115.60, 117.16, 119.73, 121.70, 129.24, 132.21, 133.76, 135.81, 146.28, 174.89. MS (ESI): m/z 410.1 $[M + Na]^+$.

(*S*)-*N*-(4-Cyano-3-(trifluoromethyl)phenyl)-2-hydroxy-2-methyl-3-(3-phenyl-1*H*-pyrrol-1-yl)propanamide (26a).: Compound **26a** was prepared following General Procedure C per Scheme 3. The product was purified by a silica gel column using ethyl acetate and hexanes (1:2) as eluents to afford 0.90 g of the titled compound as a pink solid. Yield = 62.5%. ^{1}H NMR (400 MHz, DMSO-d_6) δ: 10.41 (s, 1H, NH), 8.24 (d, J = 1.6 Hz, 1H, ArH), 8.17 (dd, J = 8.4 Hz, J = 2.0 Hz, 1H, ArH), 8.07 (d, J = 8.4 Hz, 1H, ArH), 7.38–7.33 (m, 4H, ArH), 7.28–7.24 (m, 1H, ArH), 6.96 (t, J = 3.0 Hz, 1H, pyrrole-H), 6.28 (s, 1H, OH), 6.07 (t, J = 3.5 Hz, 1H, pyrrole-H), 6.03 (m, 1H, pyrrole-H), 4.30–4.22 (m, 2H, CH_2), 1.01 (s, 3H, CH3). HRMS $[C_{22}H_{19}F_3N_3O_2^+]$: calcd 414.1429, found 414.1432 $[M + H]^+$. Analytical HPLC showed a 98.60% purity.

(*S*)-*N*-(4-Cyano-3-(trifluoromethyl)phenyl)-3-(3-(4-fluorophenyl)-1*H*-pyrrol-1-yl)-2-hydroxy-2-methylpropanamide (26b).: Compound **26b** was prepared following General Procedure C per Scheme 3. The product was purified by a silica gel column using ethyl acetate and hexanes (1:2 to 1:1) as eluents to afford 0.60 g of the titled compound as a yellowish solid. Yield = 45%. ^{1}H NMR (400 MHz, DMSO-d_6) δ: 10.40 (s, 1H, NH), 8.42 (d, J = 2.0 Hz, 1H, ArH), 8.24 (dd, J = 8.8 Hz, J = 2.0 Hz, 1H, ArH), 8.07 (d, J = 8.8 Hz, 1H, ArH), 7.43–7.38 (m, 2H, ArH), 7.11–7.05 (m, 3H, ArH), 6.73 (t, J = 2.0 Hz, 1H, pyrrole-H), 6.33–6.31 (m, 2H), 4.24 (d, J = 14.0 Hz, 1H, CH), 4.05 (d, J = 14.0 Hz, 1H, CH), 1.37 (s, 3H, CH3). HRMS $[C_{22}H_{18}F_4N_3O_2^+]$: calcd 432.1335, found 432.1331 $[M + H]^+$. Analytical HPLC showed a 99.58% purity.

(*S*)-*N*-(4-Cyano-3-(trifluoromethyl)phenyl)-3-(4-(4-fluorophenyl)-1*H*-pyrazol-1-yl)-2-hydroxy-2-methylpropanamide (26c).: Compound **26c** was prepared following General Procedure C per Scheme 3. The product was purified by a silica gel column using DCM and methanol (19:1) as eluents to afford 0.33 g of the titled compound as a white solid. Yield = 62%. ^{1}H NMR (400 MHz, DMSO-d_6) δ: 10.29 (s, 1H, NH), 8.41 (s, 1H, ArH), 8.21 (d, J = 8.8 Hz, 1H, ArH), 8.05 (d, J = 8.8 Hz, 1H, ArH), 7.68 (s, 1H, pyrazole-H), 7.61 (t, J = 6.4 Hz, 2H, ArH), 7.08 (t, J = 8.4 Hz, 2H, ArH), 6.65 (s, 1H, pyrazole-H), 6.30 (s, 1H, OH), 4.51 (d, J = 14.0 Hz, 1H, CH), 4.31 (d, J = 14.0 Hz, 1H, CH), 1.42 (s, 3H, CH_3). Mass (ESI, negative): 431.12 $[M – H]^–$; HRMS $[C_{21}H_{17}F_4N_4O_2^+]$: calcd 433.1288, found 433.1291 $[M + H]^+$. Analytical HPLC showed a 96.01% purity.

(*S*)-*N*-(4-Cyano-3-(trifluoromethyl)phenyl)-3-(5-(4-fluorophenyl)-1*H*-tetrazol-1-yl)-2-hydroxy-2-methylpropanamide (26d).: Compound **26d** was prepared following General Procedure C per Scheme 3. The product was purified by a silica gel column using DCM and ethyl acetate (9:1) as eluents to afford 0.055 g of the titled compound as a yellowish solid. Yield = 12%. ^{1}H NMR (400 MHz, DMSO-d_6) δ: 10.39 (s, 1H, NH), 8.44 (s, 1H, ArH), 8.26

(d, J = 8.2 Hz, 1H, ArH), 8.10 (d, J = 8.2 Hz, 1H, ArH), 7.93–7.89 (m, 2H, ArH), 7.30 (t, J = 8.2 Hz, 2H, ArH), 6.64 (s, 1H, OH), 5.09 (d, J = 14.0 Hz, 1H, CH), 4.92 (d, J = 14.0 Hz, 1H, CH), 1.55 (s, 3H, CH_3). Mass (ESI, negative): 433.17 $[M - H]^-$; HRMS $[C_{19}H_{15}F_4N_6O_2^+]$: calcd 435.1193, found 435.1196 $[M + H]^+$. Analytical HPLC showed a 95.12% purity.

(*S*)-*N*-(4-Cyano-3-(trifluoromethyl)phenyl)-3-((4-fluorophenyl)(phenyl)amino)-2-hydroxy-2-methylpropanamide (26e).: Compound **26e** was prepared following General Procedure C per Scheme 1. A mixture of bromide (218 mg, 0.619 mmol) and potassium carbonate (172 mg, 1.23 mmol) in 30 mL of acetone was heated to reflux for 30 min. After complete conversion of starting bromide to the desired intermediate epoxide as monitored by TLC, the solvent was evaporated under reduced pressure to give a yellowish residue, which was poured into 20 mL of anhydrous EtOAc. The solution was filtered through a celite pad to remove the K_2CO_3 residue and condensed under reduced pressure to give a yellowish solid of epoxide, which was dissolved in 5 mL of anhydrous THF to prepare a desired solution of epoxide in THF. To the solution was added 1 mL of lithium perchlorate and 4-fluoro-*N*-phenylaniline (116 mg, 0.619 mmol) in anhydrous THF (3 mL), which was cooled in an ice–water bath under an argon atmosphere. After addition, the resulting mixture was allowed to stir overnight at rt under argon. The reaction was quenched by water and then extracted with ethyl acetate. The organic layer was washed with brine, dried with $MgSO_4$, filtered, and concentrated under vacuum. The product was purified by a silica gel column using ethyl acetate and hexanes (2:1) as eluents to afford the titled compound as a brown solid. Yield = 67%. ^{1}H NMR (400 MHz, $CDCl_3$) δ: 8.85 (bs, 1H, N*H*), 7.87 (m, 1H), 7.81–7.73 (m, 2H), 7.65 (dd, J = 8.4, 1.8 Hz, 1H), 7.20 (m, 2H), 7.05–7.00 (m, 2H), 6.94–6.89 (m, 5H), 4.54 (d, J = 15.2 Hz, 1H), 3.84 (d, J = 15.2 Hz, 1H), 3.61 (s, 1H), 1.53 (s, 3H). MS (ESI, negative) 456.1 $[M - H]^-$. HRMS $[C_{24}H_{18}F_4N_3O_2^-]$: calcd 456.1335, found 456.1342 $[M - H]^-$.

(*S*)-*N*-(4-Cyano-3-(trifluoromethyl)phenyl)-3-(4-(4-fluorophenyl)-1*H*-1,2,3-triazol-1-yl)-2-hydroxy-2-methylpropanamide (26f).: Compound **26f** was prepared in two steps per Scheme 4. Step 1. A solution of **16a** (0.351 g, 1 mmol) in DMF (10 mL) was treated with NaN_3 (0.325 g, 5 mmol) under argon at 80 °C for 24 h. The reaction mixture was cooled and extracted with CH_2Cl_2 (3 × 20 mL). The combined organic layers were washed with H_2O (3 × 20 mL) and brine, dried, and evaporated to give a crude oil, which were purified by silica gel chromatography (EtOAc/*n*-hexane = 1:2, v/v) to afford 0.224 g of **27a** as a yellow solid. Yield = 72%. ^{1}H NMR (400 MHz, $CDCl_3$) δ: 9.00 (bs, 1H, NH), 8.08 (s, 1H), 7.95 (d, J = 8.4 Hz, 1H), 7.81 (d, J = 8.4 Hz, 1H), 3.92 (d, J = 12.4 Hz, 1H), 3.50 (d, J = 12.4 Hz, 1H), 2.96 (s, 1H, OH), 1.54 (s, 3H). ^{19}F NMR ($CDCl_3$, decoupled) δ: −62.21. MS (ESI) m/z 314.03 $[M + H]^+$; 312.18 $[M - H]^-$.

Step 2. To a suspension of copper(I) iodide (11 mg, 0.055 mmoL) in acetonitrile (7 mL)/water (3 mL) was added **27a** (57 mg, 0.182 mmol) at rt and then **28** (0.015 mL, 0.182 mmol) was added. The resulting reaction mixture was stirred at rt for 3 d. The mixture was evaporated under reduced pressure, poured into water/brine (1:1, v/v), and then extracted with ethyl acetate. The combined organic extracts were then washed with brine, dried over sodium sulfate, filtered, and evaporated. The product was purified by a silica gel column

using ethyl acetate and hexanes (2:3) as eluents to afford 0.052 g of the titled compound as a yellow solid. Yield = 65%. ^{1}H NMR (400 MHz, $CDCl_3$) δ: 9.07 (bs, 1H, NH), 7.82–7.80 (m, 1H), 7.79 (s, 1H), 7.76–7.74 (m, 2H), 7.72 (dd, J = 8.2, 2.8 Hz, 2H), 7.10 (t, J = 8.8 Hz, 2H), 5.15 (bs, 1H, OH), 4.96 (d, J = 14.0 Hz, 1H), 4.61 (d, J = 14.0 Hz, 1H), 1.62 (s, 3H). 19F NMR ($CDCl_3$, decoupling) δ −62.24, −112.36. HRMS [$C_{20}H_{16}F_4N_5O_2^+$]: calcd 434.1240, found 434.1256 $[M + H]^+$. Analytical HPLC showed a 99.69% purity.

(*S*)-*N*-(6-Cyano-5-(trifluoromethyl)pyridin-3-yl)-3-(4-(4-fluorophenyl)-1*H*-1,2,3-triazol-1-yl)-2-hydroxy-2-methylpropanamide (26g).: Compound **26g** was prepared in two steps per Scheme 4. Step 1. A solution of **16c** (0.352 g, 1 mmol) in DMF (10 mL) was treated with NaN_3 (0.325 g, 5 mmol) under argon at 80 °C for 24 h. The reaction mixture was cooled and extracted with CH_2Cl_2 (3 × 20 mL). The combined organic layers were washed with H_2O (3 × 20 mL) and brine, dried, and evaporated to give a crude oil, which was purified by silica gel chromatography (EtOAc/*n*-hexane = 1:2, v/v) to afford **27b** as a yellow solid. Yield = 87%. ^{1}H NMR (400 MHz, $CDCl_3$) δ: 9.16 (bs, 1H, N*H*), 8.89 (s, 1H), 8.77 (s, 1H), 3.90 (d, J = 12.0 Hz, 1H), 3.52 (d, J = 12.0 Hz, 1H), 3.20 (bs, 1H, OH), 1.55 (s, 3H). ^{19}F NMR ($CDCl_3$, decoupled) δ: −62.11. MS (ESI) m/z 314.03 $[M – H]^-$.

Step 2. To a suspension of copper(I) iodide (11 mg, 0.055 mmoL) in acetonitrile (7 mL)/water (3 mL) was added **27b** (57 mg, 0.182 mmol) at rt and then **28** (0.015 mL, 0.182 mmol) was added. The resulting reaction mixture was stirred at rt for 3 d. The mixture was evaporated under reduced pressure, poured into water/brine (1:1, v/v), and then extracted with ethyl acetate. The combined organic extracts were then washed with brine, dried over sodium sulfate, filtered, and evaporated. The product was purified by a silica gel column using ethyl acetate and hexanes (2:3) as eluents to afford 0.052 g of the titled compound as a yellow solid. Yield = 65%. ^{1}H NMR (400 MHz, $CDCl_6$) δ: 10.16 (bs, 1H, N*H*), 9.28 (s, 1H), 8.88 (s, 1H), 8.31 (s, 1H), 7.90 (t, J = 7.8 Hz, 2H), 7.20 (t, J = 8.8 Hz, 2H), 5.73 (bs, 1H, OH), 4.94 (d, J = 14.2 Hz, 1H), 4.73 (d, J = 14.2 Hz, 1H), 1.62 (s, 3H). ^{19}F NMR ($CDCl_3$, decoupling) δ −61.66, −14.58. MS (ESI) m/z 534.06 $[M + H]^+$; 433.09 $[M – H]^-$. HRMS [$C_{19}H_{13}F_4N_6O_2^-$]: calcd 433.1036, found 433.1039 $[M – H]^-$.

(*S*)-*N*-(4-Cyano-3-(trifluoromethyl)phenyl)-3-(5-(4-fluorophenyl)-1*H*-1,2,3-triazol-1-yl)-2-hydroxy-2-methylpropanamide (26h).: Compound **26h** was prepared in two steps per Scheme 4. Step 1. A solution of **16a** (0.351 g, 1 mmol) in DMF (10 mL) was treated with NaN_3 (0.325 g, 5 mmol) under argon at 80 °C for 24 h. The reaction mixture was cooled and extracted with CH_2Cl_2 (3 × 20 mL). The combined organic layers were washed with H_2O (3 × 20 mL) and brine, dried, and evaporated to give a crude oil, which were purified by silica gel chromatography (EtOAc/*n*-hexane = 1:2, v/v) to afford 0.224 g of **27a** as a yellow solid. Yield = 72%. ^{1}H NMR (400 MHz, $CDCl_3$) δ: 9.00 (bs, 1H, NH), 8.08 (s, 1H), 7.95 (d, J = 8.4 Hz, 1H), 7.81 (d, J = 8.4 Hz, 1H), 3.92 (d, J = 12.4 Hz, 1H), 3.50 (d, J = 12.4 Hz, 1H), 2.96 (s, 1H, OH), 1.54 (s, 3H). ^{19}F NMR ($CDCl_3$, decoupled) δ: −62.21. MS (ESI) m/z 314.03 $[M + H]^+$; 312.18 $[M – H]^-$.

Step 2. A mixture of **27a** (57 mg, 0.18 mmol), **28** (0.015 mL, 0.18 mmol), and copper iodide (11 mg, 0.055 mmol) in AcCN/H_2O (1/0.5 mL) was loaded into a vessel with a cap. The reaction vessels were placed in a reactor block in the microwave. A programmable

microwave irradiation cycle of 30 min on 300 W at 100 °C and 25 min off (fan-cooled) was executed two times if the starting materials were shown on TLC (total irradiation time, 60 min). The mixture was transferred to a round-bottom flask to be concentrated under reduced pressure and poured into EtOAc, which was washed with water, dried over $MgSO_4$, and concentrated. The product was purified by a silica gel column using ethyl acetate and hexanes (2:1) as eluents to afford 0.070 g of the titled compound as a yellow solid. Yield = 90%. ^{1}H NMR (400 MHz, acetone-d_6) δ: 9.00 (bs, 1H, NH), 8.44 (s, 1H), 8.30 (s, 1H), 8.25 (d, J = 8.4 Hz, 1H), 8.02 (d, J = 8.4 Hz, 1H), 7.89 (dd, J = 8.0 Hz, 2.4 Hz, 2H), 7.20 (d, J = 8.8 Hz, 2H), 5.67 (s, 1H, OH), 4.92 (d, J = 14.0 Hz, 1H), 4.72 (d, J = 14.0 Hz, 1H), 1.60 (s, 3H). ^{19}F NMR (acetone-d_6, decoupling) δ 114.68, 61.64. HRMS [$C_{20}H_{16}F_4N_5O_2^+$]: calcd 434.1240, found 434.1259 $[M + H]^+$. Analytical HPLC showed a 98.91% purity.

Biological Methods.

Competitive Ligand Binding Assay.—AR ligand binding assay was performed as described previously using the purified AR LBD cloned from rat prostate.[38,39]

AR Transactivation Assay.—HEK-293 cells plated in 24-well plates at 70 000 cells/well were transfected using Lipofectamine transfection reagent (Life Technologies, Carlsbad, CA). Cells were transfected with 0.25 μg of GRE-LUC, 25 ng of CMV-hAR, and 10 ng of CMVLUC. Cells were treated 24 h after transfection, and luciferase assay was performed 48 h after transfection. Firefly luciferase assay values were normalized to *Renilla* luciferase assay numbers.

Androgen Receptor-Dependent Gene Expression in LNCaP Cells.—LNCaP cells were plated in 96-well plates in RPMI supplemented with 1% csFBS without phenol red. Cells were maintained in this medium for 2 d and treated with the compounds in the presence of 0.1 nM R1881. Twenty-four hours after treatment, the cells were harvested, RNA was isolated, and cDNA was prepared using Cells-toct Kit (Life Technologies). Expression of genes was measured using real-time PCR using TaqMan primers and probes (Life Technologies).

Cellular Proliferation Assays in MR49F Cells.—MR49F cells were plated in 96-well plates in RPMI + 1% csFBS without phenol red. Cells were treated in this medium with the compounds in the presence of 0.1 nM R1881 for 6 d, with medium change and retreatment after 3 d. Number of viable cells was measured using Cell-Titer-Glo (Promega).

Western Blot.—Indicated cell lines were treated for 24 h. Cells were harvested, the protein was extracted, and Western blot for AR, AR SV, and GAPDH was performed using the AR PG-21 rabbit polyclonal antibody that binds to the N-terminus of the AR.[38,39]

In Vitro Metabolism Assays.—DMPK assays were performed as described before.[38,39] Metabolism assays were performed in mouse, rat, and human liver microsomes as described before.

Hershberger Assay.—Male Sprague Dawley rats (100–200 g) were randomized into groups (N = 5/group) based on body weight. Animals were orally treated with vehicle or 20

mg/kg fixed dose **26f** for 13 d. Animals were sacrificed on day 14 of treatment, and seminal vesicle organs were removed and weighed. Organ weights were normalized to body weight.

Xenograft Studies.—Enzalutamide-resistant LNCaP cells (5 million/mouse: 1:1 medium:Matrigel) were implanted subcutaneously in male NSG mice. Once the tumors reach 200–400 mm^3, the animals were castrated, and the tumors were allowed to regrow as castration-resistant prostate cancer (CRPC). Once the regrown tumors reached 400 mm^3, the animals were randomized and treated orally with vehicle or 60 mg/kg/day **26f**. Tumor volume was measured twice weekly. Animals were sacrificed 28 d after treatment, and the tumors were processed for further analysis. $*p < 0.05$.

Animal Studies.—All animal studies were conducted under the UTHSC Animal Care and Use Committee-approved protocols and in accordance with the UTHSC guidelines.

Supplementary Material

Refer to Web version on PubMed Central for supplementary material.

ACKNOWLEDGMENTS

The authors thank GTx, Inc. and Oncternal Therapeutics, Inc. for supporting this project and Dr. Dejian Ma of UTHSC, College of Pharmacy, for assistance with HPLC purity and HRMS experiments.

Funding

The work in this manuscript was funded in part by a research grant from GTx, Inc. and Oncternal Therapeutics, Inc. (R.N. and D.D.M.), by a research grant from National Cancer Institute (NCI) to R.N. (1R01CA229164), and by a grant from the University of Tennessee Health Science Center (UTHSC) for Cancer Research (R.N. and D.D.M.).

ABBREVIATIONS

ADT	androgen deprivation therapy
AF-1	an activation function
AF-2	an external (solvent exposed) binding site termed activation function-2
AR	androgen receptor
AR SV	AR splice variant
CRPC	castration-resistant prostate cancer
csFBS	charcoal-stripped fetal bovine serum
CSPC	castration-sensitive PC
DBD	DNA-binding domain
DHT	5α-dihydrotestosterone
DMPK	distribution, metabolism, and pharmacokinetic

EnzR	enzalutamide-resistant
ER	estrogen receptor
FL	full length
GR	glucocorticoid receptor
GRE	glucocorticoid response element
LBD	ligand binding domain
MIB	milbolerone
MLM	mouse liver microsomes
NSG	NOD SCID γ
NTD	N-terminal domain
PC	prostate cancer
PD	pharmacodynamics
PK	pharmacokinetic
PR	progesterone receptor
PROTACs	proteolysis-targeting chimaeras
RLUs	relative light units
rt	room temperature
SAR	structure–activity relationship
SARDs	selective androgen receptor degraders
SARM	selective androgen receptor modulator
TGI	tumor growth inhibition
UPS	ubiquitin proteasome system
VP	ventral prostate
wt	wild type

REFERENCES

(1). Aragon-Ching JB The Evolution of Prostate Cancer Therapy: Targeting the Androgen Receptor. Front. Oncol 2014, 4, 1–3. [PubMed: 24478982]

(2). Siegel RL; Miller KD; Jemal A Cancer statistics, 2015. Ca-Cancer J. Clin 2015, 65, 5–29. [PubMed: 25559415]

(3). Chen CD; Welsbie DS; Tran C; Baek SH; Chen R; Vessella R; Rosenfeld MG; Sawyers CL Molecular determinants of resistance to antiandrogen therapy. Nat. Med 2004, 10, 33–39. [PubMed: 14702632]

(4). Torre LA; Bray F; Siegel RL; Ferlay J; Lortet-tieulent J; Jemal A Global Cancer Statistics, 2012. Ca-Cancer J. Clin 2015, 65, 87–108. [PubMed: 25651787]

(5). Tian X; He Y; Zhou J Progress in antiandrogen design targeting hormone binding pocket to circumvent mutation based resistance. Front. Pharmacol 2015, 6, No. 57. [PubMed: 25852559]

(6). Barradell LB; Faulds D Cyproterone. A review of its pharmacology and therapeutic efficacy in prostate cancer. Drugs Aging 1994, 5, 59–80. [PubMed: 7919640]

(7). Neumann F The antiandrogen cyproterone acetate: discovery, chemistry, basic pharmacology, clinical use and tool in basic research. Exp. Clin. Endocrinol. Diabetes 1994, 102, 1–32.

(8). Delaere KP; Van Thillo EL Flutamide Monotherapy as Primary Treatment in Advanced Prostatic Carcinoma. Semin. Oncol 1991, 18, 13–18. [PubMed: 1948117]

(9). Kolvenbag GJ; Blackledge GR; Gotting-Smith K Bicalutamide (Casodex) in the Treatment of Prostate Cancer: History of Clinical Development. Prostate 1998, 43, 61–72.

(10). Scher HI; Beer TM; Higano CS; Anand A; Taplin ME; Efstathiou E; Rathkopf D; Shelkey J; Yu EY; Alumkal J; Hung D; Hirmand M; Seely L; Morris MJ; Danila DC; Humm J; Larson S; Fleisher M; Sawyers CL Antitumour Activity of MDV3100 in Castration-Resistant Prostate Cancer: A Phase 1–2 Study. Lancet 2010, 375, 1437–1446. [PubMed: 20398925]

(11). Chong JT; Oh WK; Liam BC Profile of apalutamide in the treatment of metastatic castration-resistant prostate cancer: evidence to date. OncoTargets Ther. 2018, 11, 2141–2147.

(12). Dellis AE; Rapatsois AG Apalutamide: The established and emerging roles in the treatment of advanced prostate cancer. Expert Opin. Invest. Drugs 2018, 27, 553–559.

(13). Sugawara T; Baumgart SJ; Nevedomskaya E; Reichert K; Steuber H; Lejeune P; Mumberg D; Haendler B Darolutamide is a potent androgen receptor antagonist with strong efficacy in prostate cancer models. Int. J. Cancer 2019, 145, 1382–1394. [PubMed: 30828788]

(14). Bastos DA; Antonarakis ES Darolutamide For Castration-Resistant Prostate Cancer. OncoTargets Ther. 2019, 12, 8769–8777.

(15). Attard G; Reid AH; Auchus RJ; Hughes BA; Cassidy AM; Thompson E; Oommen NB; Folkerd E; Dowsett M; Arlt W; de Bono JS Clinical and biochemical consequences of CYP17A1 inhibition with abiraterone given with and without exogenous glucocorticoids in castrate men with advanced prostate cancer. J. Clin. Endocrinol. Metab 2012, 97, 507–516. [PubMed: 22170708]

(16). Chi KN; Agarwal N; Bjartell A; Chung BH; Pereira de Santana Gomes AJ; Given R; Juarez Soto A; Merseburger AS; Ozguroglu M; Uemura H; Ye D; Deprince K; Naini V; Li J; Cheng S; Yu MK; Zhang K; Larsen JS; McCarthy S; Chowdhury S; TITAN Investigators. Apalutamide for Metastatic, Castration-Sensitive Prostate Cancer. N. Engl. J. Med 2019, 381, 13–24. [PubMed: 31150574]

(17). Nuhn P; De Bono JS; Fizazi K; Freedland SJ; Grilli M; Kantoff PW; Sonpavde G; Sternberg CN; Yegnasubramanian S; Antonarakis ES Update on Systemic Prostate Cancer Therapies: Management of Metastatic Castration-resistant Prostate Cancer in the Era of Precision Oncology. Eur. Urol 2019, 75, 88–99. [PubMed: 29673712]

(18). Kwan EM; Thangasamy IA; Teh J; Alghazo O; Sathianathen NJ; Lawrentschuk N; Azad AA Navigating systemic therapy for metastatic castration-naive prostate cancer. World J. Urol 2021, 39, 339–348. [PubMed: 31897602]

(19). Harris WP; Mostaghel EA; Nelson PS; Montgomery B Androgen deprivation therapy: progress in understanding mechanisms of resistance and optimizing androgen depletion. Nat. Clin. Pract. Urol 2009, 6, 76. [PubMed: 19198621]

(20). Eileen Tan MH; Li J; Xu HE; Melcher K; Yong E.-l. Androgen receptor: structure, role in prostate cancer and drug discovery. Acta Pharmacol. Sin 2015, 36, 3. [PubMed: 24909511]

(21). Visakorpi T; Hyytinen E; Koivisto P; Tanner M; Keinänen R; Palmberg C; Palotie A; Tammela T; Isola J; Kallioniemi O-P In vivo amplification of the androgen receptor gene and progression of human prostate cancer. Nat. Genet 1995, 9, No. 401. [PubMed: 7795646]

(22). Linja MJ; Savinainen KJ; Saramäki OR; Tammela TLJ; Vessella RL; Visakorpi T Amplification and Overexpression of Androgen Receptor Gene in Hormone-Refractory Prostate Cancer. Cancer Res. 2001, 61, 3550–3555. [PubMed: 11325816]

(23). Yamaoka M; Hara T; Kusaka M Overcoming Persistent Dependency on Androgen Signaling after Progression to Castration-Resistant Prostate Cancer. Clin. Cancer Res 2010, 16, 4319–4324. [PubMed: 20647476]

(24). Veldscholte J; Ris-Stalpers C; Kuiper GG; Jenster G; Berrevoets C; Claassen E; van Rooij HC; Trapman J; Brinkmann AO; Mulder E A Mutation in the Ligand Binding Domain of the Androgen Receptor of Human LNCaP Cells Affects Steroid Binding Characteristics and Response to Anti-Androgens. Biochem. Biophys. Res. Commun 1990, 173, 534–540. [PubMed: 2260966]

(25). Grasso CS; Wu Y-M; Robinson DR; Cao X; Dhanasekaran SM; Khan AP; Quist MJ; Jing X; Lonigro RJ; Brenner JC; Asangani IA; Ateeq B; Chun SY; Siddiqui J; Sam L; Anstett M; Mehra R; Prensner JR; Palanisamy N; Ryslik GA; Vandin F; Raphael BJ; Kunju LP; Rhodes DR; Pienta KJ; Chinnaiyan AM; Tomlins SA The mutational landscape of lethal castration-resistant prostate cancer. Nature 2012, 487, 239. [PubMed: 22722839]

(26). Scher HI; Sayers CL Biology of Progressive, Castration-Resistant Prostate Cancer: Directed Therapies Targeting the Androgen-Receptor Signaling Axis. J. Clin. Oncol 2005, 23, 2854–2861.

(27). Gregory CW; He B; Johnson RT; Ford OH; Mohler JL; French FS; Wilson EM A Mechanism for Androgen Receptor-mediated Prostate Cancer Recurrence after Androgen Deprivation Therapy. Cancer Res. 2001, 61, 4315–4319. [PubMed: 11389051]

(28). Wen Y; Hu MC; Makino K; Spohn B; Bartholomeusz G; Yan DH; Hung MC HER-2/neu promotes androgen-independent survival and growth of prostate cancer cells through the Akt pathway. Cancer Res. 2000, 60, 6841. [PubMed: 11156376]

(29). Majumder PK; Seller WR Akt-regulated pathways in prostate cancer. Oncogene 2005, 24, 7465–7474. [PubMed: 16288293]

(30). Ueta T; Sadar MD; Suzuki H; Akakura K; Sakamoto S; Shimbo M; Suyama T; Imamoto T; Komiya A; Yukio N; Ichikawa T Interleukin-4 in Patients with Prostate Cancer. Anticancer Res. 2005, 25, 4595–4598. [PubMed: 16334148]

(31). Ueda T; Mawji NR; Bruchovsky N; Sadar MD Ligand-independent activation of the androgen receptor by interleukin-6 and the role of steroid receptor coactivator-1 in prostate cancer cells. J. Biol. Chem 2002, 277, 38087–38094. [PubMed: 12163482]

(32). Culig Z; Hobisch A; Cronauer MV; Radmayr C; Trapman J; Hittmair A; Bartsch G; Klocke rH. Androgen receptor activation in prostatic tumor cell lines by insulin-like growth factor-I, keratinocyte growth factor, and epidermal growth factor. Cancer Res. 1994, 54, 5447–5448.

(33). Antonarakis ES; Chandhasin C; Osbourne E; Luo J; Sadar MD; Perabo F Targeting the N-Terminal Domain of the Androgen Receptor: A New Approach for the Treatment of Advanced Prostate Cancer. Oncologist 2016, 21, 1427–1435. [PubMed: 27628492]

(34). Dutt SS; Gao AC Molecular mechanisms of castration-resistant prostate cancer progression. Future Oncol. 2009, 5, 1403–1413. [PubMed: 19903068]

(35). Scher HI; Sawyers CL Biology of Progressive, Castration-Resistant Prostate Cancer: Directed Therapies Targeting the Androgen-Receptor Signaling Axis. J. Clin. Oncol 2005, 23, 8253–8261. [PubMed: 16278481]

(36). De Maeseneer DJ; Van Praet C; Lumen N; Rottey S Battling resistance mechanisms in antihormonal prostate cancer treatment: Novel agents and combinations. Urol. Oncol.: Semin. Orig. Invest 2015, 33, 310–321.

(37). Ito Y; Sadar MD Enzalutamide and blocking androgen receptor in advanced prostate cancer: lessons learnt from the history of drug development of antiandrogens. Res. Rep. Urol 2018, 10, 23–32. [PubMed: 29497605]

(38). Ponnusamy S; Coss CC; Thiyagarajan T; Watts K; Hwang DJ; He Y; Selth LA; McEwan IJ; Duke CB; Pagadala J; Singh G; Wake RW; Ledbetter C; Tilley WD; Moldoveanu T; Dalton JT; Miller DD; Narayanan R Novel Selective Agents for the Degradation of Androgen Receptor Variants to Treat Castration-Resistant Prostate Cancer. Cancer Res. 2017, 77, 6282–6298. [PubMed: 28978635]

(39). Hwang DJ; He Y; Ponnusamy S; Mohler ML; Thiyagarajan T; McEwan IJ; Narayanan R; Miller DD New Generation of Selective Androgen Receptor Degraders: Our Initial Design, Synthesis, and Biological Evaluation of New Compounds with Enzalutamide-Resistant Prostate Cancer Activity. J. Med. Chem 2019, 62, 491–511. [PubMed: 30525603]

(40). Ponnusamy S; He Y; Hwang DJ; Thiyagarajan T; Houtman R; Bocharova V; Sumpter BG; Fernandez E; Johnson D; Du Z; Pfeffer LM; Getzenberg RH; McEwan IJ; Miller DD; Narayanan R Orally Bioavailable Androgen Receptor Degrader, Potential Next-Generation Therapeutic for Enzalutamide-Resistant Prostate Cancer. Clin. Cancer Res 2019, 25, 6764–6780. [PubMed: 31481513]

(41). Mohler ML; Bohl CE; Jones A; Coss CC; Narayanan R; He Y; Hwang DJ; Dalton JT; Miller DD Nonsteroidal selective androgen receptor modulators (SARMs): dissociating the anabolic and androgenic activities of the androgen receptor for therapeutic benefit. J. Med. Chem 2009, 52, 3597–3617. [PubMed: 19432422]

(42). He Y; Yin D; Perera M; Kirkovsky L; Stourman N; Li W; Dalton JT; Miller DD Novel nonsteroidal ligands with high binding affinity and potent functional activity for the androgen receptor. Eur. J. Med. Chem 2002, 37, 619–634. [PubMed: 12161060]

(43). Clegg NJ; Wongvipat J; Joseph JD; Tran C; Ouk S; Dilhas A; Chen Y; Grillot K; Bischoff ED; Cai L; Aparicio A; Dorow S; Arora V; Shao G; Qian J; Zhao H; Yang G; Cao C; Sensintaffar J; Wasielewska T; Herbert MR; Bonnefous C; Darimont B; Scher HI; Smith-Jones P; Klang M; Smith ND; De Stanchina E; Wu N; Ouerfelli O; Rix PJ; Heyman RA; Jung ME; Sawyers CL; Hager JH ARN-509: a novel antiandrogen for prostate cancer treatment. Cancer Res. 2012, 72, 1494–1503. [PubMed: 22266222]

(44). Okegawa T; Ninomiya N; Masuda K; Nakamura Y; Tambo M; Nutahara K AR-V7 in circulating tumor cells cluster as a predictive biomarker of abiraterone acetate and enzalutamide treatment in castration-resistant prostate cancer patients. Prostate 2018, 78, 576–582. [PubMed: 29508425]

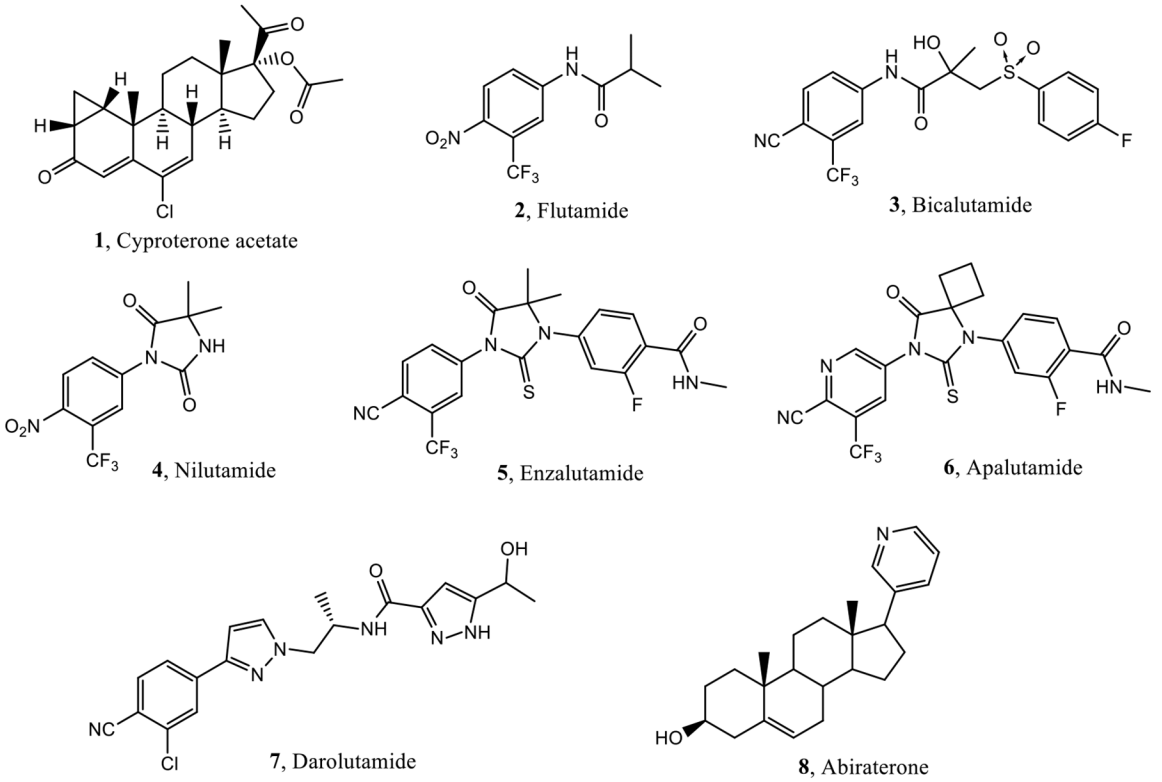

Figure 1.

Overview of known androgen receptor antagonists. Clinically approved agents include steroidal antiandrogen (**1**), first-generation (**2**–**4**) second-generation (**5**–**7**) antiandrogens, as well as an indirect androgen synthesis inhibitor (**8**).

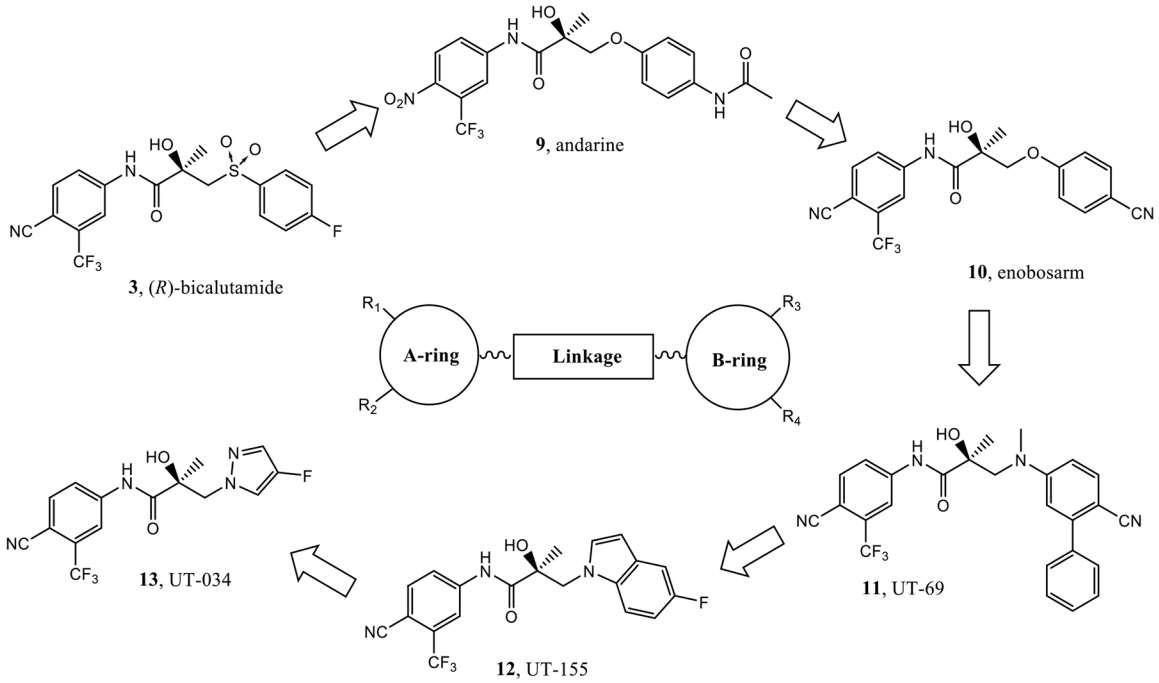

Figure 2.

Clinical selective androgen receptor modulators (SARMs) (**9** and **10**) and preclinical SARDs (**11**–**13**). A series of diaryl propanamides form the basis for a nonsteroidal general pharmacophore for AR binding that consists of A-ring–linkage–B-ring structural elements. The arrows below indicate the evolution of propanamide AR ligands over time.

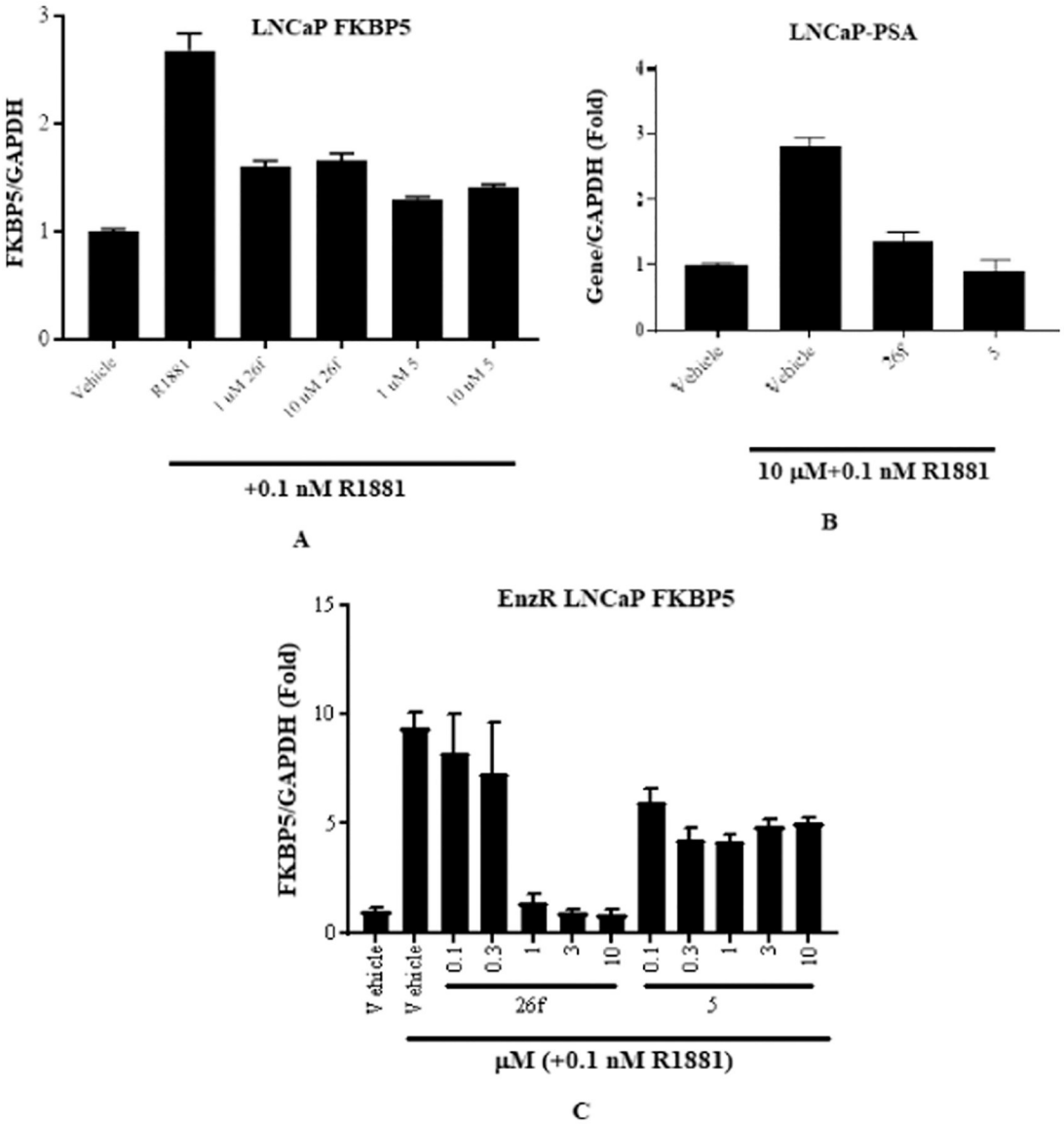

Figure 3.

(A) **26f** antagonizes AR function in LNCaP prostate cancer cells. LNCaP cells were maintained for 2 d in a charcoal-stripped fetal bovine serum (csFBS)-containing medium. The cells were treated with antagonists, as indicated in the figure, for 20–24 h, RNA was isolated, and expression of AR target gene, *FKBP5*, was measured and normalized to GAPDH using real-time polymerase chain reaction (PCR). (B) **26f** antagonizes AR function in LNCaP prostate cancer cells. LNCaP cells were maintained in a csFBS-containing medium for 2 d. The medium was changed and treated as indicated with 10 *μM* **26f** in the presence of 0.1 nM R1881. Cells were harvested 24 h after treatment, and expression of PSA was measured by real-time PCR and normalized to GAPDH. (C) Enzalutamide (**5**)-resistant (EnzR) LNCaP cells (MR49F) were plated in 96-well plates in a 1% csFBS-containing medium. Cells were maintained in this medium for 2 days and treated as indicated in the

figure. RNA was extracted, and real-time PCR for FKBP5 was performed and normalized to GAPDH expression.

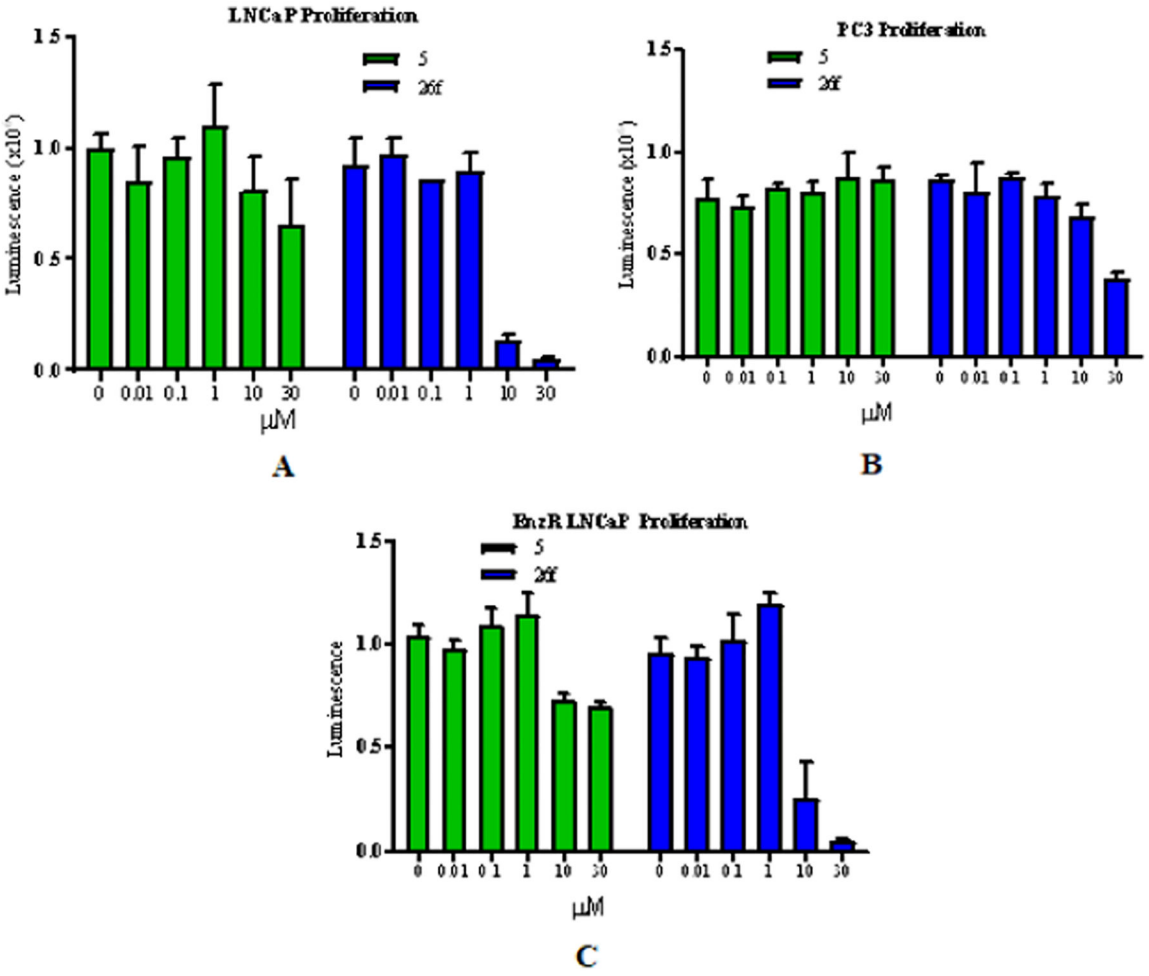

Figure 4.

(A) LNCaP cellular antiproliferation. LNCaP cells were plated and treated in a 1% charcoal-stripped serum-containing medium with the indicated doses of the compounds in the presence of 0.1 nM R1881. Cells were treated for 6 d with medium change and retreated after 3 d. Cell-Titer-Glo assay was performed to determine the viable cells. (B) PC3 cellular proliferation. PC3 cells were plated and treated in a 1% charcoal-stripped serum-containing medium with the indicated doses of the compounds. Cells were treated for 6 d with medium change and retreated after 3 d. Cell-Titer-Glo assay was performed to determine the viable cells. (C) Enzalutamide-resistant LNCaP (MR49F) cellular antiproliferation. Enzalutamide (**5**)-resistant (EnzR) LNCaP cells (MR49F cells) were plated and treated in a 1% charcoal-stripped serum-containing medium with the indicated doses of the compounds in the presence of 0.1 nM R1881. Cells were treated for 6 d with medium change and retreatment after 3 d. Cell-Titer-Glo assay was performed to determine the viable cells.

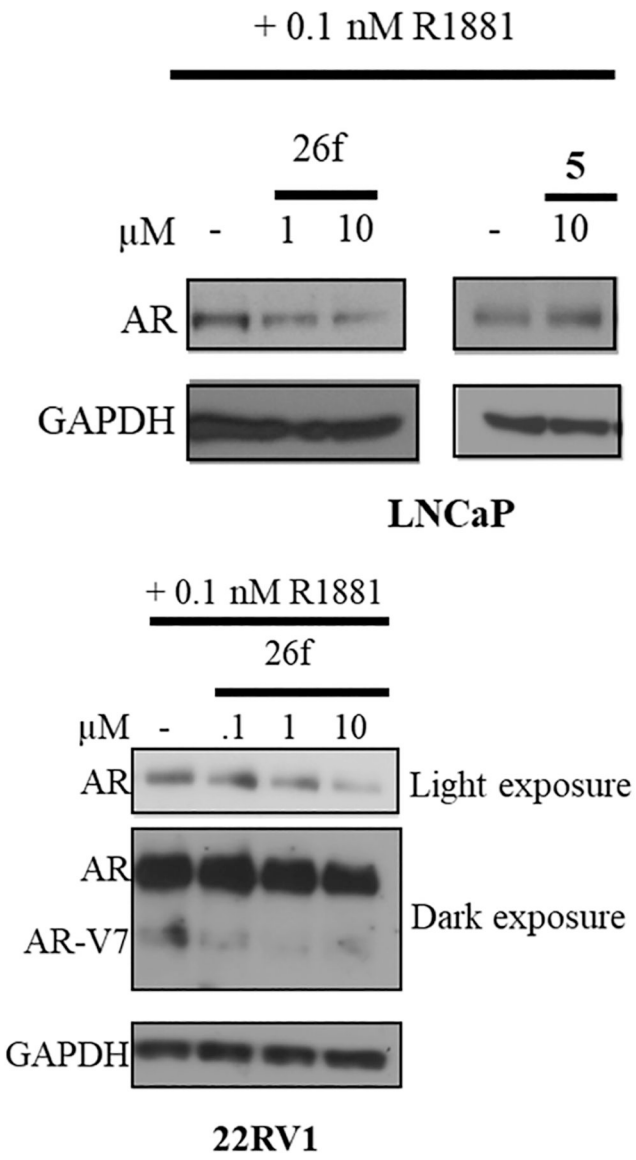

Figure 5.

26f degrades enzalutamide (**5**) resistance-conferring escape mutant AR. EnzR LNCaP cells (MR49F cells) (top panel) or 22RV1 cells (bottom panel) were maintained in a charcoal-stripped serum-containing medium for 2 d and treated with 0.1 nM R1881 (agonist) and a titration of the **26f** or **5**, as indicated in the figure. Twenty-four hours after treatment, cells were harvested and the protein was extracted and blotted with an AR-N20 antibody. Blots were stripped and reprobed with a GAPDH antibody.

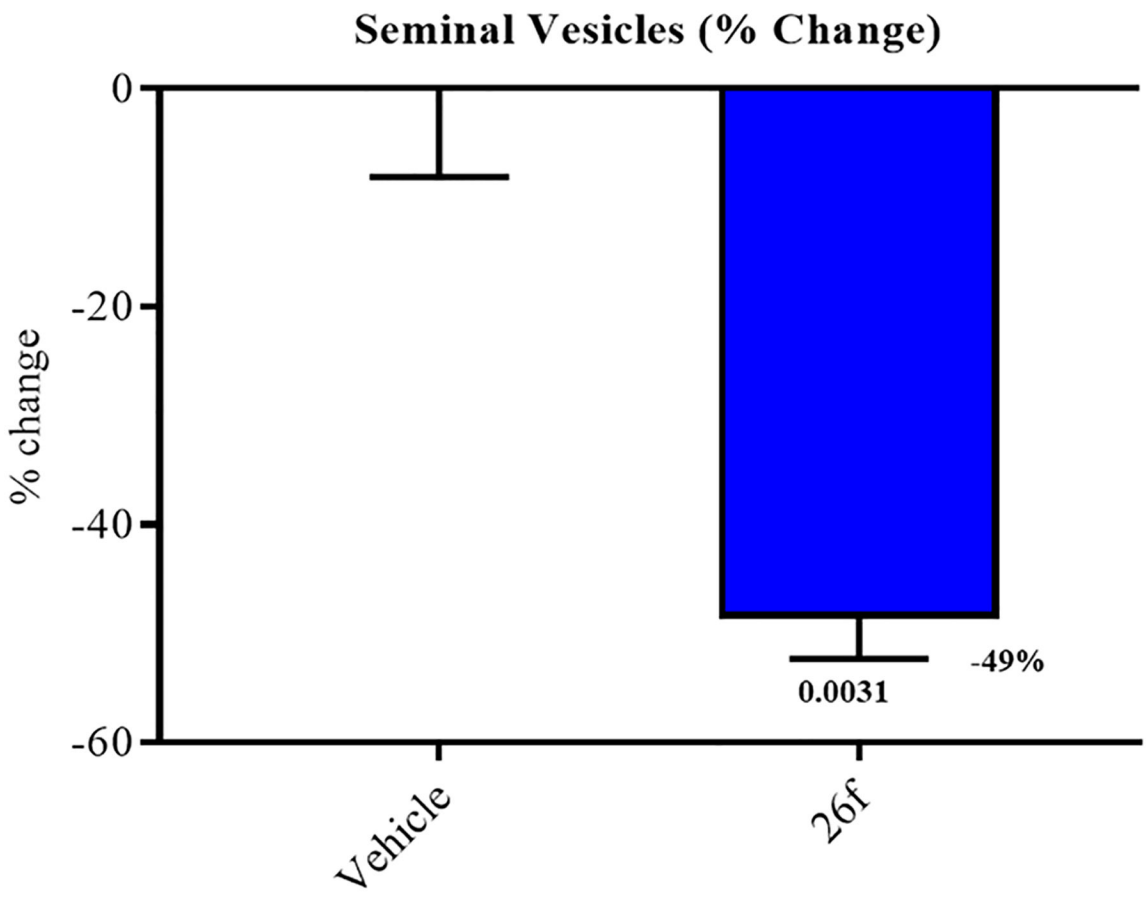

Figure 6.

SARDs and pan-antagonists inhibit androgen-dependent organs in rats. Male Sprague Dawley rats (100–120 g) were treated orally with vehicle or 20 mg/kg **26f** for 13 d. Animals were sacrificed on the 14th day, and seminal vesicle weights were recorded. The inhibition of the seminal vesicle growth measured as loss of organ weight by **26f** vs vehicle was statistically significant ($p = 0.0031$). $N = 5$/group.

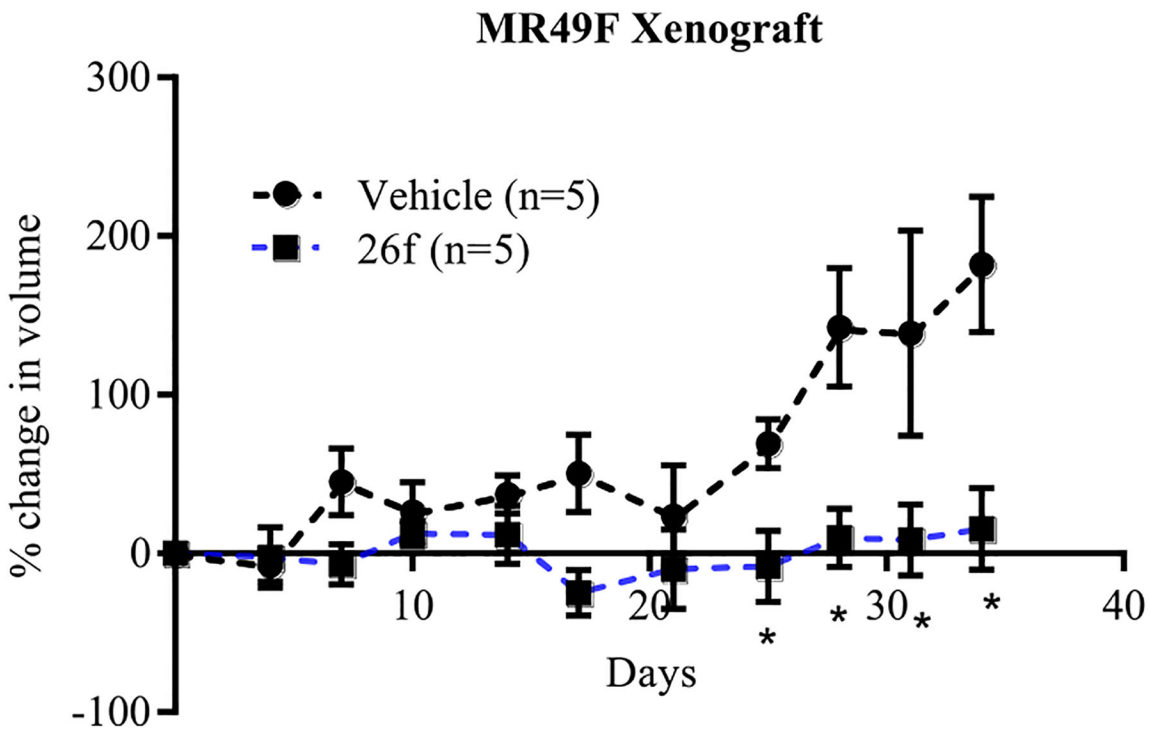

Figure 7.

26f inhibits the growth of enzalutamide (**5**)-resistant prostate cancer. EnzR LNCaP (MR49F) cells (5 million/mouse: 1:1 medium/Matrigel) were implanted subcutaneously in male NSG mice. Once the tumors reach 200–400 mm^3, the animals were castrated, and the tumors were allowed to regrow as castration-resistant prostate cancer (CRPC). Once the regrown tumors reach 400 mm^3, the animals were randomized and treated orally with vehicle or 60 mg/kg/day **26f**. Tumor volume was measured twice weekly. Animals were sacrificed 28 d after treatment, and the tumors were processed for further analysis. * $p < 0.05$.

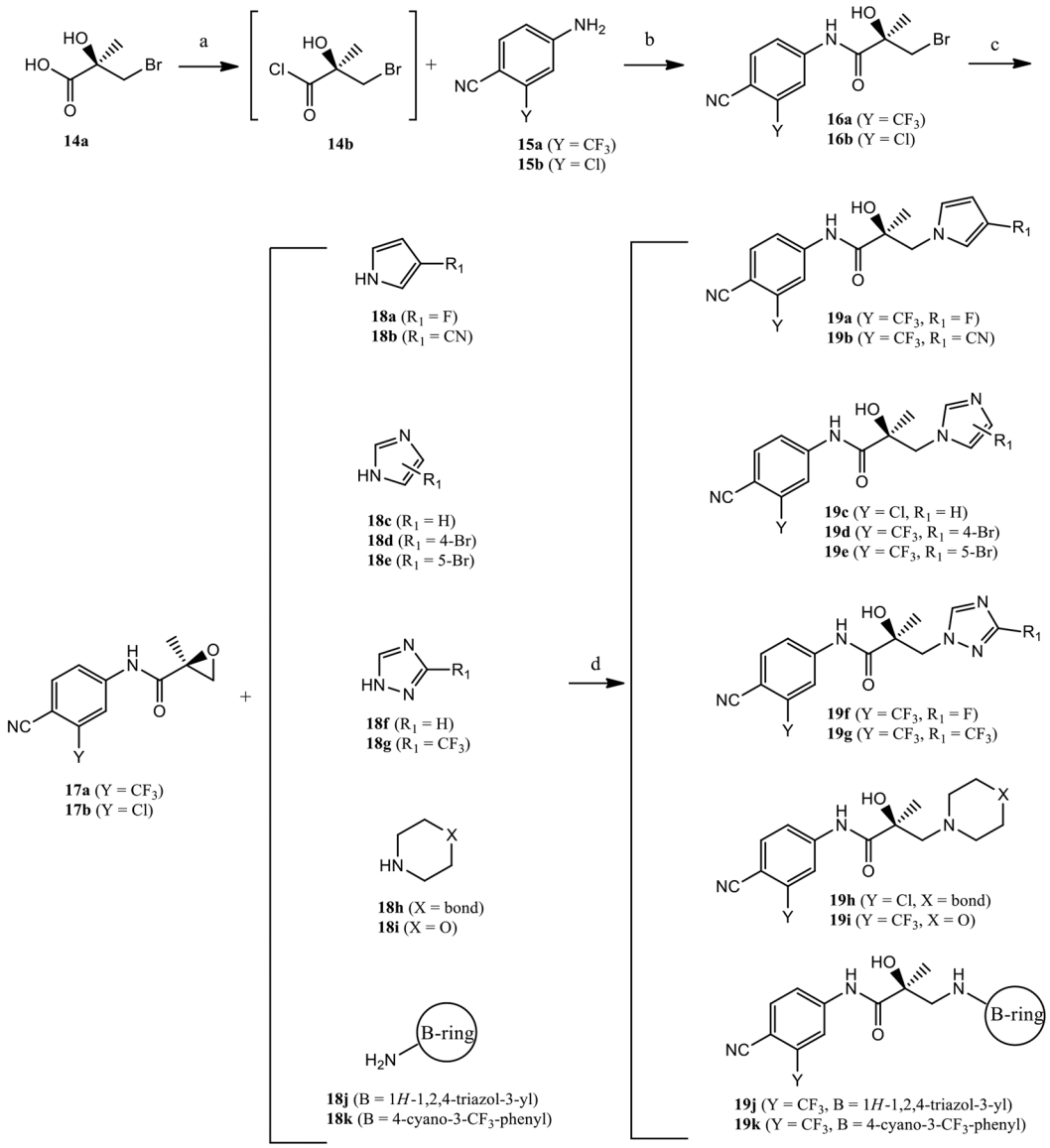

Scheme 1.

Synthesis of Compounds 19a–k[a]

[a]Reagents and conditions: (a) $SOCl_2$ in tetrahydrofuran (THF), −10 to 0 °C; (b) Et_3N in THF, −10 to 0 °C, and then to 50 °C, 2–3 h; (c) 2-butanone, K_2CO_3, reflux; and (d) NaH in THF, 0 °C to room temperature.

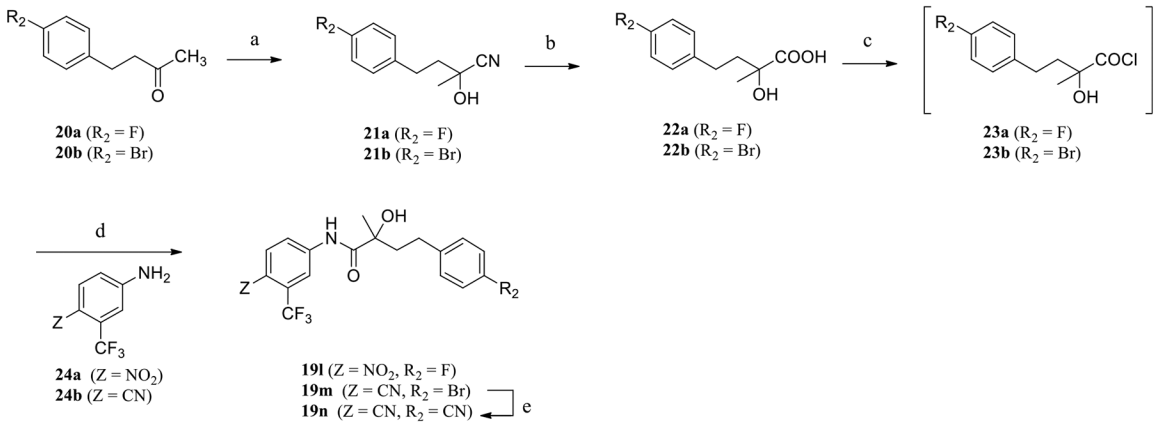

Scheme 2.

Synthesis of Compounds 19l–n[a]

[a]Reagents and conditions: (a) Me_3SiCN, ZnI_2 dichloromethane (DCM); (b) HCl, reflux; (c) $SOCl_2$ in THF, −10 to 0 °C; (d) Et_3N in THF, reflux 12 h; and (e) Cu(I)CN, microwave irradiation at 150 °C in dimethylformamide (DMF).

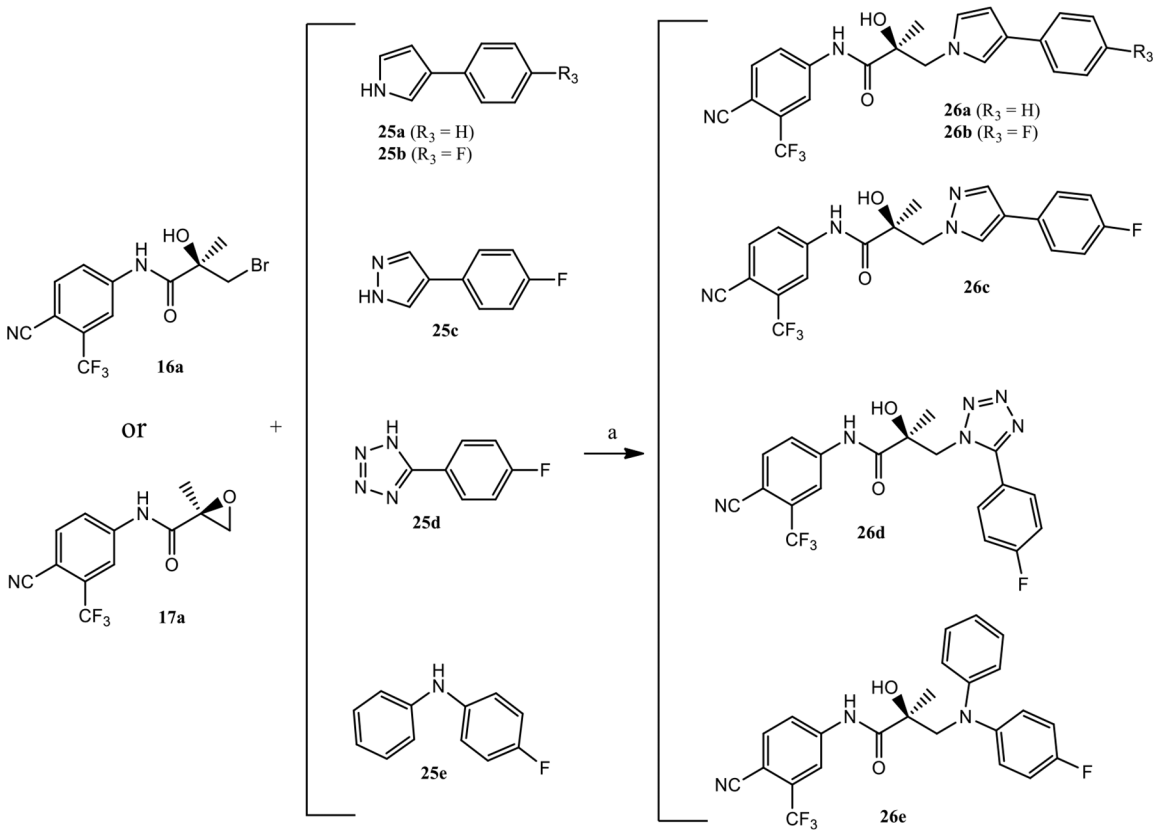

Scheme 3.

Synthesis of Compounds 26a–e[a]

[a]Reagents and conditions: (a) NaH in THF, 0 °C to room temperature.

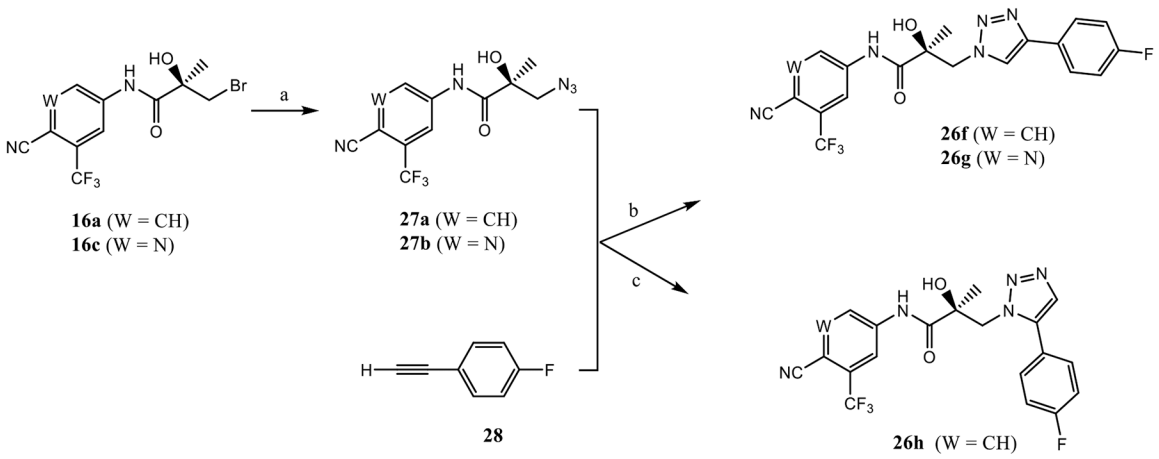

Scheme 4.

Synthesis of Compounds 26f–h[a]

[a]Reagents and conditions: (a) NaN_3 in DMF, 80 °C, 24 h; (b) the copper(I)-catalyzed azide–alkyne cycloaddition (CuAAC)/Cu(I)I, in acetonitrile/H_2O, room temperature, 3 d; and (c) Huisgen cycloaddition: heat, in acetonitrile/H_2O.

Table 1.

AR Binding and Antagonistic Activity of Propanamide Derivatives (13, 19a–n) with Monocyclic B-Ring Modifications

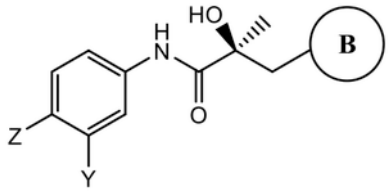

Compound ID	B-ring	Binding (K_i) / Transactivation (IC_{50}) (μM)		SARD Activity (% degradation)	
		K_i (DHT=1nM)[a]	IC_{50}[b]	Full Length[c] (LNCaP) at 1 μM	Splice Variant[c] (22RV1) at 10 μM
13 (Y=CF_3; Z=CN)[d]	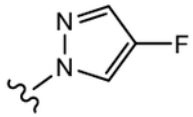	>10	0.199	100	100
19a (Y=CF_3; Z=CN)	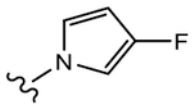	0.633	Partial agonist[e]	0	0
19b (Y=CF_3; Z=CN)	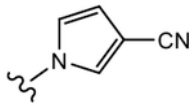	0.328	Partial agonist	0	0
19c (Y=Cl; Z=CN)	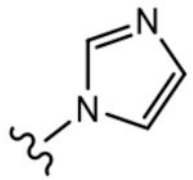	>10	1.856	0	30

Compound ID	B-ring	Binding (K_i) / Transactivation (IC_{50}) (μM)		SARD Activity (% degradation)	
		K_i (DHT=1nM)[a]	IC_{50}[b]	Full Length[c] (LNCaP) at 1 μM	Splice Variant[c] (22RV1) at 10 μM
19d (Y=CF_3; Z=CN)		0.906	0.149 Partial agonist	0	0
19e (Y=CF_3; Z=CN)		>10	1.019	50	70
19f (Y=CF_3; Z=CN)		>10	1.091	0	0
19g (Y=CF_3; Z=CN)		>10	1.013	68	100

Compound ID	B-ring	Binding (K_i) / Transactivation (IC_{50}) (μM)		SARD Activity (% degradation)	
		K_i (DHT=1nM)[a]	IC_{50}[b]	Full Length[c] (LNCaP) at 1 μM	Splice Variant[c] (22RV1) at 10 μM
19h (Y=Cl; Z=CN)		>10	No effect	0	0
19i (Y=CF_3; Z=CN)		1.874	1.018	52	80
19j (Y=CF_3; Z=CN)		>10	No effect	0	N.A.[f]
19k (Y=CF_3; Z=CN)		>10	Agonist	0	N.A.
19l (Y=CF_3; Z=NO_2)		N.A.	Agonist	N.A.	N.A.

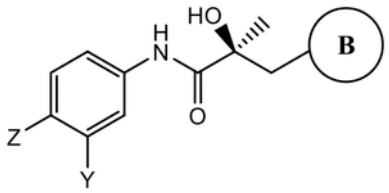

Compound ID	B-ring	Binding (K_i) / Transactivation (IC_{50}) (μM)		SARD Activity (% degradation)	
		K_i (DHT=1nM)[a]	IC_{50}[b]	Full Length[c] (LNCaP) at 1 μM	Splice Variant[c] (22RV1) at 10 μM
19m (Y=CF_3; Z=CN)	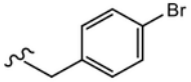	0.251	Agonist	N.A.	N.A.
19n (Y=CF_3; Z=CN)	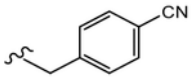	0.884	Agonist	N.A.	N.A.

[a] AR binding was determined by competitive binding of 1 nM tritiated mibolerone ([^{3}H] MIB) to recombinant LBD of wild-type AR (wtAR). DHT was used in each experiment as a standard agent, and the values are normalized to DHT, with the IC_{50} of DHT taken as 1 nM.

[b] Inhibition of transactivation was determined by transfecting HEK-293 or COS-7 cells with full-length wtAR, GRE-LUC, and CMV-renilla luciferase for transfection control. Cells were treated 24 h after transfection with a dose–response of compounds (1 pM–10 μM) in the presence of 0.1 nM R1881 (antagonist mode) or in the absence of R1881 (agonist mode). Luciferase assay was performed 24 h after treatment using a dual luciferase (firefly and *Renilla*) assay kit (Promega, Madison, WI and Goldbio Luciferase kit, St. Louis, MO).

[c] SARD activity was assayed by treating LNCaP or 22RV1 cells for determining FL AR (at 1 μM of antagonist) or AR SV (at 10 μM of antagonist) protein levels, respectively. Cells were maintained in a charcoal-stripped serum-containing medium for 48 h and treated with the indicated doses of antagonist for 24 h in the presence of 0.1 nM R1881 (agonist). Cells were harvested, and Western blot for AR was performed using AR-N20 or PG-21 antibody that is directed toward the NTD of AR and actin (internal control for protein loading). The AR FL and AR SV bands were quantified and normalized to actin bands and represented as percent inhibition from vehicle-treated cells.

[d] The result was reported in the literature in the same assay as described here.[40]

[e] Transcriptional activation was performed in the same assay in agonist mode.

[f] N.A. means data not available.

Table 2.

AR Binding and Antagonistic Activity of Propanamide Derivatives (26a–h) with Biaryl or Diaryl B-Ring Modifications

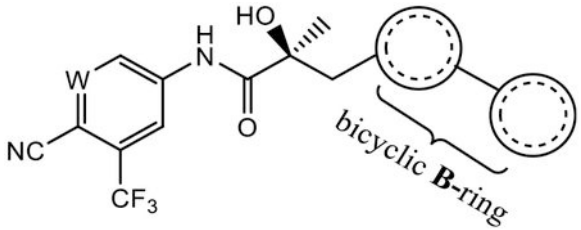

Compound (W)	B-ring	Binding (K_i) / Transactivation (IC_{50}) (μM)		SARD Activity (% degradation)	
		K_i (DHT=lnM)[a]	IC_{50}[a]	Full Length[a] (LNCaP) at 1 μM	Splice Variant[a] (22RV1) at 10 μM
11 (C)[b]	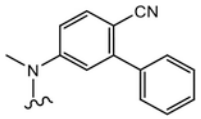	0.078	0.048[c]	70,100[d]	71–100
12 (C)[c]	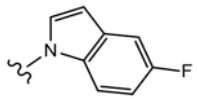	0.267	0.085	65–83	60–100
26a (C)	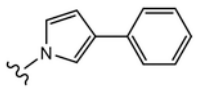	0.322	0.178 Partial	0, 40[d]	0
26b (C)	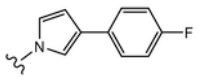	0.259	0.226	100	60
26c (C)	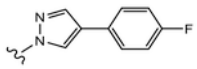	0.612	0.969	60	0

Compound (W)	B-ring	Binding (K_i) / Transactivation (IC_{50}) (μM)		SARD Activity (% degradation)	
		K_i (DHT=1nM)[a]	IC_{50}[a]	Full Length[a] (LNCaP) at 1 μM	Splice Variant[a] (22RV1) at 10 μM
26d (C)		N.A.[e]	No effect	N.A.	N.A.
26e (C)		0.275	0.172	42	16
26f (C)		>10	0.383	84	74
26g (N)		1.486	0.217	12	0
26h (C)		0.703	0.317	73	N.A.
3 (bicalutamide)[c]		0.509	0.248	-	-

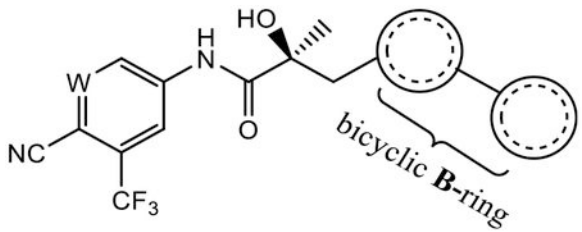

Compound (W)	B-ring	Binding (K_i) / Transactivation (IC_{50}) (μM)		SARD Activity (% degradation)	
		K_i (DHT=lnM)[a]	IC_{50}[a]	Full Length[a] (LNCaP) at 1 μM	Splice Variant[a] (22RV1) at 10 μM
5 (enzalutamide)[c]		3.641	0.216	-	-

[a] AR binding, transactivation, and degradation assays were performed, and values are reported, as described in Table 1.

[b] The compound was reported in the literature in the same assay as described here.[40]

[c] The result was reported in the literature in the same assay as described here.[38,40]

[d] The two values indicate SARD assays run with 1 and 10 μM of antagonist.

[e] N.A. means data not available.

Table 3.

In Vitro Metabolic Stability for Selected Compounds in Mouse Liver Microsomes (MLMs)

	(DMPK) MLM[a]	
compound ID	**$T_{1/2}$ (min)**	**CL_{int} (mL/min/mg)**
11 [b]	1.15	208.8
12 [b]	12.11	57.26
13 [b]	77.96	0.89
19c	24.61	28.16
19e	26.51	41.58
26a	3.96	157.5
26b	17.93	38.66
26e	5.07	136.8
26f	265	2.67
26h	>360	~0
5 (enzalutamide)	10.04 h[c]	86.3[d]

[a] Compounds were incubated together with mouse liver microsomes (MLMs) with cofactors for phases I and II provided, as described in the Experimental Section.

[b] Reported previously using the same method as in the Experimental Section.[38,40]

[c] $T_{1/2}$ (h) after oral administration in humans as previously reported in ref 43.

[d] CL (mL/h/kg) after oral administration in humans as previously reported.[43]